

Article

Bioceramics Based on β -Calcium Pyrophosphate

Tatiana Safronova ^{1,2,*}, Andrey Kiselev ¹, Irina Selezneva ³, Tatiana Shatalova ^{1,2}, Yulia Lukina ^{4,5}, Yaroslav Filippov ^{2,6}, Otabek Toshev ², Snezhana Tikhonova ², Olga Antonova ⁷ and Alexander Knotko ²

- ¹ Department of Chemistry, Lomonosov Moscow State University, Building, 3, Leninskie Gory, 1, 119991 Moscow, Russia; artes915@yandex.ru (A.K.); shatalovtb@gmail.com (T.S.)
 - ² Department of Materials Science, Lomonosov Moscow State University, Building, 73, Leninskie Gory, 1, 119991 Moscow, Russia; filippovyy@my.msu.ru (Y.F.); otabetoshev0995@mail.ru (O.T.); kurbatova.snezhana@yandex.ru (S.T.); knotko@inorg.chem.msu.ru (A.K.)
 - ³ Institute of Theoretical and Experimental Biophysics, Russian Academy of Sciences, Institutskaya, 3, 142290 Pushchino, Russia; selezneva_i@mail.ru
 - ⁴ Priorov National Medical Research Center of Traumatology and Orthopedics, Priorova, 10, 127299 Moscow, Russia; lukinayus@cito-priorov.ru
 - ⁵ Department of Engineering Design of Technological Equipment, Mendeleev University of Chemical Technology, Miusskaya, 9, 125047 Moscow, Russia
 - ⁶ Research Institute of Mechanics, Lomonosov Moscow State University, Michurinsky, 1, 119192 Moscow, Russia
 - ⁷ Baikov Institute of Metallurgy and Material Science, Russian Academy of Sciences, Leninsky, 49, 119334 Moscow, Russia; oantonova@imet.ac.ru
- * Correspondence: safronovtv@my.msu.ru; Tel.: +7-(916)3470641



Citation: Safronova, T.; Kiselev, A.; Selezneva, I.; Shatalova, T.; Lukina, Y.; Filippov, Y.; Toshev, O.; Tikhonova, S.; Antonova, O.; Knotko, A. Bioceramics Based on β -Calcium Pyrophosphate. *Materials* **2022**, *15*, 3105. <https://doi.org/10.3390/ma15093105>

Academic Editor: Gigliola Lusvardi

Received: 20 February 2022

Accepted: 19 April 2022

Published: 25 April 2022

Publisher's Note: MDPI stays neutral with regard to jurisdictional claims in published maps and institutional affiliations.



Copyright: © 2022 by the authors. Licensee MDPI, Basel, Switzerland. This article is an open access article distributed under the terms and conditions of the Creative Commons Attribution (CC BY) license (<https://creativecommons.org/licenses/by/4.0/>).

Abstract: Ceramic samples based on β -calcium pyrophosphate β -Ca₂P₂O₇ were prepared from powders of γ -calcium pyrophosphate γ -Ca₂P₂O₇ with preset molar ratios Ca/P = 1, 0.975 and 0.95 using firing at 900, 1000, and 1100 °C. Calcium lactate pentahydrate Ca(C₃H₅O₃)₂·5H₂O and monocalcium phosphate monohydrate Ca(H₂PO₄)₂·H₂O were treated in an aqua medium in mechanical activation conditions to prepare powder mixtures with preset molar ratios Ca/P containing calcium hydrophosphates with Ca/P = 1 (precursors of calcium pyrophosphate Ca₂P₂O₇). These powder mixtures containing calcium hydrophosphates with Ca/P = 1 and non-reacted starting salts were heat-treated at 600 °C after drying and disaggregation in acetone. Phase composition of all powder mixtures after heat treatment at 600 °C was presented by γ -calcium pyrophosphate γ -Ca₂P₂O₇ according to the XRD data. The addition of more excess of monocalcium phosphate monohydrate Ca(H₂PO₄)₂·H₂O (with appropriate molar ratio of Ca/P = 1) to the mixture of starting components resulted in lower dimensions of γ -calcium pyrophosphate (γ -Ca₂P₂O₇) individual particles. The grain size of ceramics increased both with the growth in firing temperature and with decreasing molar ratio Ca/P of powder mixtures. Calcium polyphosphate ($t_{\text{melt}} = 984$ °C), formed from monocalcium phosphate monohydrate Ca(H₂PO₄)₂·H₂O, acted similar to a liquid phase sintering additive. It was confirmed by tests in vitro that prepared ceramic materials with preset molar ratios Ca/P = 1, 0.975, and 0.95 and phase composition presented by β -calcium pyrophosphate β -Ca₂P₂O₇ were biocompatible and could maintain bone cells proliferation.

Keywords: calcium lactate pentahydrate; monocalcium phosphate monohydrate; mechanical activation; powder; brushite; monetite; calcium pyrophosphate; ceramics; biocompatibility

1. Introduction

Ceramics based on calcium phosphates are widely used for bone defect treatment [1,2]. Resorbable calcium phosphate ceramic materials are necessary for the implementation of bone defect treating methods of regenerative medicine [3]. It is known from the scientific literature that the ability of inorganic materials to resorb is connected with the ability to

solve in an aqua medium [4]; this ability to a great extent depends on the crystal structure of an inorganic substance [5]. Calcium phosphate's ability to solve in an aqua medium can be enhanced by decreasing Ca/P molar ratio [6]. At the same time pH generated during the dissolution of calcium phosphate has to be close to neutral as a necessary feature of biocompatibility [7]. So, the ceramics based on calcium pyrophosphate $\text{Ca}_2\text{P}_2\text{O}_7$ can be an interesting object of investigation both due to molar ratio $\text{Ca}/\text{P} = 1$ (it is less than molar ratio $\text{Ca}/\text{P} = 1.67$ for insoluble hydroxyapatite $\text{Ca}_{10}(\text{PO}_4)_6(\text{OH})_2$ and $\text{Ca}/\text{P} = 1.5$ for tricalcium phosphate $\text{Ca}_3(\text{PO}_4)_2$) and due to pH close to neutral ($\text{pH} \sim 7$) during immersion to the water [8].

According to the information from scientific literature ceramics based on β -calcium pyrophosphate or ceramics containing phase of β -calcium pyrophosphate have repeatedly been the subject of investigation dealing with creation of materials for bone defect treatment [9–13]. In all these technics different powder precursors were used.

Different powders and powder mixtures with molar ratio $\text{Ca}/\text{P} = 1$ can be used as precursors of high-temperature β -modification of calcium pyrophosphate $\text{Ca}_2\text{P}_2\text{O}_7$ as the ceramic phase. Powders of brushite $\text{CaHPO}_4 \cdot 2\text{H}_2\text{O}$ [9], monetite CaHPO_4 [10], hydrated amorphous calcium pyrophosphate $\text{Ca}_2\text{P}_2\text{O}_7 \cdot x\text{H}_2\text{O}$ [11,12], calcium pyrophosphate $\text{Ca}_2\text{P}_2\text{O}_7$ in forms of γ or β modifications [13,14], can be used as starting direct powder precursors for β -calcium pyrophosphate β - $\text{Ca}_2\text{P}_2\text{O}_7$ ceramics preparation.

Solid-state sintering of calcium phosphate ceramics has some difficulties due to the complexity of mass-transfer because of the lower diffusion of the large, multiply charged phosphate or pyrophosphate ions [15]. It is impossible to help sintering of calcium pyrophosphate ceramics with elevating of firing temperature because of β - α phase transition at 1150°C [16]. Using fine powders, special atmospheres of firing, and sintering additives can enhance the sintering ability of any ceramic material. Chemical synthesis of calcium phosphate powders for ceramic preparation is used for enhancement of powder sintering activity [17]. CO_2 or H_2O atmosphere can intensify the sintering of hydroxyapatite [18]. Sintering additives with the ability to introduce defects in the crystal structure can help solid-state sintering [19,20]. Quite an ordinary decision to overcome the difficulties in sintering of calcium phosphate ceramics consists in using liquid phase sintering [21]. Liquid phase sintering can be realized when the sintering additive is presented in a quantity of a wide interval from 1% to 40%. Sodium phosphates [22,23], sodium carbonate [24], sodium/potassium nitrates [25], and calcium polyphosphate [9,26,27] were used as sintering additives for calcium pyrophosphate ceramic preparation. Potassium carbonate [28,29], potassium chloride [30], and calcium chloride [31] used as sintering additives for ceramic based on hydroxyapatite can also be used as sintering additives for calcium pyrophosphate ceramics. It should be noted, that in investigations [26,27], calcium polyphosphate was introduced in preceramic samples prepared as cement stone via excess of monocalcium phosphate monohydrate. Application of low temperature melting salts with biocompatible cations such as potassium or sodium has a slight disadvantage, which consists in the possibility of the drift of phase composition of bioceramics to the oxide systems $\text{Na}_2\text{O}-\text{CaO}-\text{P}_2\text{O}_5$ or $\text{K}_2\text{O}-\text{CaO}-\text{P}_2\text{O}_5$ and the formation of phases of double phosphates due to heterophase reactions. The possibility of these reactions can lead to the diminution of the quantity of sintering additive when processing ceramics, and then formation in ceramics of those phases of double phosphates, which, in case of notable amount, can generate basic pH harmful for a patient organism if implanted. Ceramic materials in the $\text{CaO}-\text{P}_2\text{O}_5$ system with low content of $\text{Ca}(\text{PO}_3)_2$ as expected will be more friendly to the living organism if implanted.

As precursors of the calcium polyphosphate phase in ceramics, the different compounds can be used [32]. The following compounds with molar ratio $\text{Ca}/\text{P} = 0.5$ also can be used as precursors of calcium polyphosphate: amorphous hydrated calcium polyphosphate $\text{Ca}(\text{PO}_3)_2 \cdot x\text{H}_2\text{O}$ [33], $\text{CaH}_2(\text{HPO}_3)_2$ [34], $\text{CaH}_2\text{P}_2\text{O}_7$ [35], $\text{CaH}_2\text{P}_2\text{O}_7 \cdot \text{H}_2\text{O}$ [36], $\text{CaNH}_4\text{HP}_2\text{O}_7$ [37,38], $\text{Ca}(\text{NH}_4)_2\text{P}_2\text{O}_7 \cdot \text{H}_2\text{O}$ [39,40], $\text{CaNH}_4\text{HP}_2\text{O}_7$, $\text{Ca}_2\text{NH}_4\text{H}_3(\text{P}_2\text{O}_7)_2 \cdot \text{H}_2\text{O}$, $\text{Ca}_2\text{NH}_4\text{H}_3(\text{P}_2\text{O}_7)_2 \cdot 3\text{H}_2\text{O}$ [41], $\text{Ca}(\text{H}_2\text{PO}_4)_2$, and $\text{Ca}(\text{H}_2\text{PO}_4)_2 \cdot \text{H}_2\text{O}$ [42,43].

Earlier, it was shown that the synthesis of fine grain powder of monetite CaHPO_4 can be carried out in conditions of mechanical activation from powder mixture including hydroxyapatite $\text{Ca}_{10}(\text{PO}_4)_6(\text{OH})_2$ and monocalcium phosphate monohydrate $\text{Ca}(\text{H}_2\text{PO}_4)_2 \cdot \text{H}_2\text{O}$ [10]. It also was shown that treatment in a water solution of lactic acid allowed preparing powder of monocalcium phosphate monohydrate $\text{Ca}(\text{H}_2\text{PO}_4)_2 \cdot \text{H}_2\text{O}$ with lower dimensions of particles as far lactic acid can act as a surface-active substance [44]. It is well known that the smaller the particle dimensions of starting components the more homogeneous powder mixture can be prepared. So, in the present work, powder mixtures for ceramics production were prepared in the first time in conditions of mechanical activation from calcium lactate pentahydrate $\text{Ca}(\text{C}_3\text{H}_5\text{O}_3)_2 \cdot 5\text{H}_2\text{O}$ and monocalcium phosphate monohydrate $\text{Ca}(\text{H}_2\text{PO}_4)_2 \cdot \text{H}_2\text{O}$ when the last was taken in excess and used also as a precursor of calcium polyphosphate $\text{Ca}(\text{PO}_3)_2$ which played the role of a liquid phase sintering additive.

The aim of the present work consisted in the preparation of β -calcium pyrophosphate ceramics with the assistance of calcium polyphosphate as a liquid phase sintering additive based on fine synthetic powders of γ -calcium pyrophosphate with Ca/P molar ratios preset as 1, 0.975, 0.95 and investigation of biocompatibility of prepared ceramics in vitro.

2. Materials and Methods

2.1. Materials

Powders of calcium lactate pentahydrate $\text{Ca}(\text{C}_3\text{H}_5\text{O}_3)_2 \cdot 5\text{H}_2\text{O}$ (CAS no. 814-80-2, food-grade E327 of FCC, Henan Jindan Lactic Acid Technology Co., Ltd., Zhengzhou, Henan, China) and monocalcium phosphate monohydrate $\text{Ca}(\text{H}_2\text{PO}_4)_2 \cdot \text{H}_2\text{O}$ (CAS no. 10031-30-8, puriss. 99%, Product of Spain, Sigma-Aldrich Chemie GmbH, Steinheim, Germany) were used for powder mixtures preparation.

The target phase compositions of ceramics are shown in Table 1. Calcium polyphosphate was introduced as a sintering additive with a low melting point (984 °C [16]).

Table 1. Description of target phase composition of ceramics.

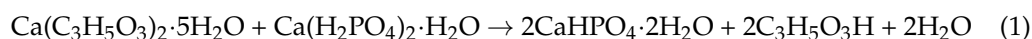
Sample	Ca/P Molar Ratio	The Phase Composition, mol. %		The Phase Composition, mas. %	
		$\beta\text{-Ca}_2\text{P}_2\text{O}_7$	$\beta\text{-Ca}(\text{PO}_3)_2$	$\beta\text{-Ca}_2\text{P}_2\text{O}_7$	$\beta\text{-Ca}(\text{PO}_3)_2$
Pyro	1	100	0	100	0
Pyro_05Poly	0.975	95	5	96	4
Pyro_10Poly	0.95	90	10	92	8

Compositions of powder mixtures before treatment in mechanical activation conditions are presented in Table 2.

Table 2. Composition of powder mixtures before treatment in mechanical activation conditions.

Sample	Ca/P Molar Ratio	Starting Components, mol. %		Starting Components, mas. %	
		$\text{Ca}(\text{C}_3\text{H}_5\text{O}_3)_2 \cdot 5\text{H}_2\text{O}$	$\text{Ca}(\text{H}_2\text{PO}_4)_2 \cdot \text{H}_2\text{O}$	$\text{Ca}(\text{C}_3\text{H}_5\text{O}_3)_2 \cdot 5\text{H}_2\text{O}$	$\text{Ca}(\text{H}_2\text{PO}_4)_2 \cdot \text{H}_2\text{O}$
Pyro	1	50.0	50.0	55.0	45.0
Pyro_05Poly	0.975	48.7	51.3	53.7	46.3
Pyro_10Poly	0.95	47.4	52.6	52.4	47.6

Reaction (1) corresponding to powder mixture “Pyro” was used to calculate quantities of starting components.



2.2. Powder Mixtures Preparation

A total 10 g of starting components in ratios are presented in Table 2; 50 g of grinding media made from zirconia and 40 mL of distilled water were placed in containers made

from zirconia. Containers with starting components were fixed in the planetary mill (Fritch Pulverisette, Idar-Oberstein, Germany). Mechanical activation of suspension initially containing distilled water, calcium lactate pentahydrate $\text{Ca}(\text{C}_3\text{H}_5\text{O}_3)_2 \cdot 5\text{H}_2\text{O}$, and monocalcium phosphate monohydrate $\text{Ca}(\text{H}_2\text{PO}_4)_2 \cdot \text{H}_2\text{O}$ was conducted for 15 min at a rotation speed of 600 rpm. Then, powder mixtures after drying for a week were disaggregated in a planetary mill in acetone medium for 15 min at a rotation speed of 600 rpm. After drying powder mixtures were passed through the sieve with 200 μm mesh. Then, powder mixtures were heat-treated at 600 °C for 30 min.

2.3. Ceramic Samples Preparation

Powder mixtures prepared as described above were used for ceramics preparation. Powder compacts were pressed at 100 MPa in the form of disks with a diameter of 12 mm and height of 1 mm in steel mold using the manual press (Carver Laboratory Press model C, Fred S. Carver, Inc., Wabash, IN, USA). Then, powder compacts were fired in the air at 900, 1000, and 1100 °C with a heating rate of 5 °C/min and 2 h holding at a specified temperature.

2.4. Characterization Methods

The phase composition of the prepared powder mixtures, powders after heat treatment at 600 °C, and ceramic samples after firing was determined by X-ray powder diffraction (XRD) analysis using Rigaku D/Max-2500 diffractometer (Rigaku Corporation, Tokyo, Japan) with a rotating anode (Cu-K α radiation), angle interval 2θ : from 2° to 70°, step $2\theta - 0.02^\circ$. Phase analysis was performed using the ICDD PDF2 database [45]

Thermal analysis (TA) was performed to determine the total mass loss of the powder mixtures at heating up to 1000 °C in the air using NETZSCH STA 449 F3 Jupiter thermal analyzer (NETZSCH, Selb, Germany). The gas-phase composition was monitored by the quadrupole mass spectrometer QMS 403 Quadro (NETZSCH, Selb, Germany) combined with a thermal analyzer NETZSCH STA 449 F3 Jupiter. The mass spectra (MS) were registered for the following m/z values: 18 (H_2O); 44 (CO_2); the heating rate was 10 °C/min.

Powders after heat treatment at 600 °C and ceramics after firing were examined by scanning electron microscopy (SEM) on a LEO SUPRA 50VP electron microscope (Carl Zeiss, Jena, Germany; auto-emission source). This investigation was carried out at an accelerating voltage of 3–20 kV using SE2 detectors. The surface of the ceramic samples and powders was coated with a layer of chromium (up to 10 nm).

2.5. Biocompatibility Estimation

Ceramic samples fired at 1100 °C were used for the investigation of biocompatibility *in vitro*.

Primary dental pulp stem cells (cell culture) were used to study the biocompatibility of the prepared ceramics. The dental pulp stem cells culture was obtained from freshly extracted third molar teeth (donor age, 16 years) with a root at least two-thirds formed, which were extracted for orthodontics reasons [46]. The cell cultures were maintained in DMEM/F12 medium supplemented with 10% FBS, 100 units mL^{-1} penicillin, and 100 mg mL^{-1} streptomycin under an 80% humidity with 5% CO_2 atmosphere at 37 °C.

For assessing cytotoxicity of ceramics direct contact method was used. The samples were placed onto 24-well culture plates. The cells were seeded on the surfaces of ceramic samples at 40,000 cell cm^{-2} and cultured in DMEM/F12 (1:1) medium supplemented with 10% FBS, 100 units mL^{-1} penicillin, and 100 mg mL^{-1} streptomycin at 80% humidity in a 5% CO_2 atmosphere at 37 °C. The cytotoxicity of the ceramic samples was estimated by evaluating the cell viability through a double-staining fluorescence assay in a direct contact procedure 2 and 7 days after the beginning of experiments. In this study, the ability of the prepared ceramics to support the adhesion of the primary dental pulp stem cells and to stimulate their proliferation was also examined. We used a double-staining assay with SYTO9 (green fluorescent nucleic acid stain), which stains all cells, and propidium iodide (red

fluorescent nucleic acid stain), which stains the nuclei of dead cells (L-7007 LIVE/DEAD Bac Light Bacterial Viability Kit, Invitrogen, Thermo Fisher Scientific, Eugene, USA). The cells were visualized using fluorescence microscopy (Axiovert 200, Zeiss, Germany).

The cell-containing surfaces of prepared ceramic specimens after primary dental pulp stem cells cultivation were studied using a Tescan Vega II scanning electron microscope (SEM, Tescan Vega II, Brno, Czech Republic); the imaging was performed in a low vacuum mode at an accelerating voltage of 20 kV (SE detector). To prepare samples of the cell-containing surfaces of ceramics after 2 days of cells cultivation for SEM analysis, the cells were fixed and dehydrated. Briefly, the samples were washed three times with PBS and fixed with glutaraldehyde (2.5% in PBS, pH 7.4) for 2 h. After fixation, the samples were rinsed with PBS once before being dehydrated using a series of solutions. Samples were coated with a thin layer of gold to prevent surface charging (Q150R ES, Quorum Technologies, East Sussex, UK).

The cytotoxicity of the ceramics was evaluated using the MTT test according to ISO 10993-5. The samples were incubated in polypropylene tubes containing DMEM/F12 supplemented with 100 U mL^{-1} penicillin/streptomycin for 3 days at 37°C under aseptic conditions. In the liquid extracts of materials, the ratio of the mass of the samples (g) to the volume of the culture medium (mL) was 0.1–0.2. DMEM/F12 medium was used as a control. The NCTC L929 cells were used at $40,000 \text{ cells cm}^{-2}$ for 24 h before adding the liquid extracts of the material. The extracts were transferred onto a layer of cells and incubated. The viability of the cells was evaluated 1 day after the beginning of experiments by measuring the reduction of the colorless salt tetrazolium(3-[4,5-dimethylthiazol-2-yl]-2,5-diphenyltetrazolium bromide) (MTT) by mitochondrial and cytoplasmic dehydrogenases of living metabolically active cells through the formation of intracellular water-insoluble purple-blue crystals of formazan. The cells were treated with MTT (0.5 mg mL^{-1}) at 37°C for 3 h in air with 5% CO_2 and 90% humidity. The medium was removed and the formazan was solubilized with $100 \mu\text{L}$ dimethylsulfoxide (DMSO). The absorption at 540 nm was measured using a microplate spectrophotometer (model 680 BioRad, Bio-Rad Laboratories, Inc., Hercules, CA, USA). The value was an average of three separate experiments. The results for the optical densities were expressed as mean standard deviation. The statistically significant difference between the groups was estimated using the Mann–Whitney U test. Differences at $p < 0.05$ were considered statistically significant.

3. Results and Discussion

According to XRD analysis (Figure 1), after homogenization of starting salts in mechanical activation conditions in a planetary mill in aqua medium powder mixture “Pyro” (Ca/P = 1) included brushite $\text{CaHPO}_4 \cdot 2\text{H}_2\text{O}$; monetite CaHPO_4 in small quantity; and starting components, i.e., calcium lactate pentahydrate $\text{Ca}(\text{C}_3\text{H}_5\text{O}_3)_2 \cdot 5\text{H}_2\text{O}$ and monocalcium phosphate monohydrate $\text{Ca}(\text{H}_2\text{PO}_4)_2 \cdot \text{H}_2\text{O}$. Powder mixtures “Pyro_05Poly” (Ca/P = 0.975) and “Pyro_10Poly” (Ca/P = 0.95) included monetite CaHPO_4 and starting components, i.e., calcium lactate pentahydrate $\text{Ca}(\text{C}_3\text{H}_5\text{O}_3)_2 \cdot 5\text{H}_2\text{O}$ and monocalcium phosphate monohydrate $\text{Ca}(\text{H}_2\text{PO}_4)_2 \cdot \text{H}_2\text{O}$. The presence of starting salts in all powder mixtures under investigation can be explained by the incompleteness of the reactions (1). Moreover, monocalcium phosphate monohydrate $\text{Ca}(\text{H}_2\text{PO}_4)_2 \cdot \text{H}_2\text{O}$ was intentionally introduced in powder mixtures “Pyro_05Poly” (Ca/P = 0.975) and “Pyro_10Poly” (Ca/P = 0.95) in excess to provide formation of calcium polyphosphate $\text{Ca}(\text{PO}_3)_2$ at the firing stage. An intentionally introduced excess of monocalcium phosphate monohydrate $\text{Ca}(\text{H}_2\text{PO}_4)_2 \cdot \text{H}_2\text{O}$ provided more acidic pH of water solution formed during treatment of powder mixtures “Pyro_05Poly” (Ca/P = 0.975) and “Pyro_10Poly” (Ca/P = 0.95) in a planetary mill. More acidic pH of water solution, as shown before in other investigations [47,48], can explain the preferable formation of monetite CaHPO_4 (calcium hydrophosphate anhydrate) in powder mixtures “Pyro_05Poly” (Ca/P = 0.975) and “Pyro_10Poly” (Ca/P = 0.95) instead of brushite $\text{CaHPO}_4 \cdot 2\text{H}_2\text{O}$ (calcium hydrophosphate dihydrate) as it was for powder mixture “Pyro”.

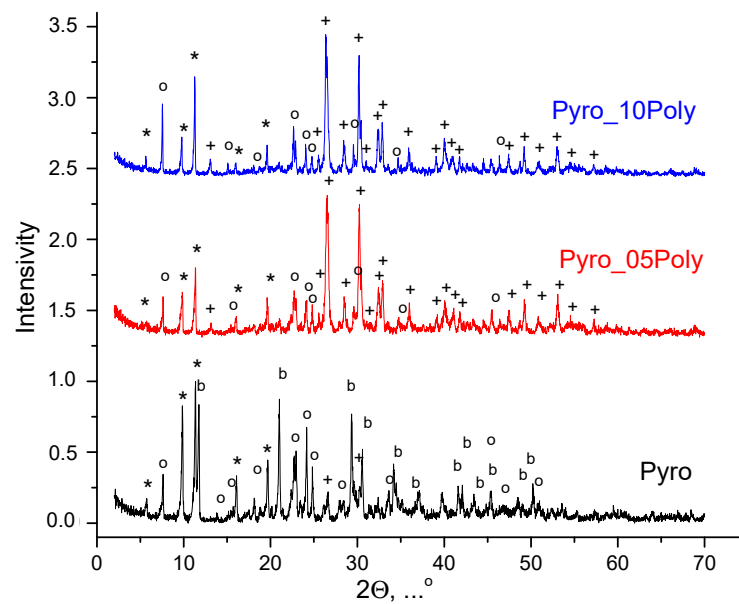
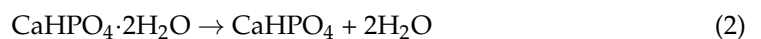


Figure 1. XRD data for powder mixtures prepared in mechanical activation conditions from calcium lactate pentahydrate $\text{Ca}(\text{C}_3\text{H}_5\text{O}_3)_2 \cdot 5\text{H}_2\text{O}$ and monocalcium phosphate monohydrate $\text{Ca}(\text{H}_2\text{PO}_4)_2 \cdot \text{H}_2\text{O}$: *— $\text{Ca}(\text{C}_3\text{H}_5\text{O}_3)_2 \cdot 5\text{H}_2\text{O}$ (according to scientific literature data [49–51]); o— $\text{Ca}(\text{H}_2\text{PO}_4)_2 \cdot \text{H}_2\text{O}$ (PDF card 9-347); +— CaHPO_4 (PDF card 9-80); b— $\text{CaHPO}_4 \cdot 2\text{H}_2\text{O}$ (PDF card 9-77).

After drying, the prepared powder mixtures were aggregated to a great extent and the stage of disaggregation was highly necessary. So, after drying powder mixtures were disaggregated in acetone medium in a planetary mill. According to XRD data (Figure 2), after disaggregation in acetone medium in planetary mill, phase composition of all powder mixtures included monetite CaHPO_4 and starting components, i.e., calcium lactate pentahydrate $\text{Ca}(\text{C}_3\text{H}_5\text{O}_3)_2 \cdot 5\text{H}_2\text{O}$ and monocalcium phosphate monohydrate $\text{Ca}(\text{H}_2\text{PO}_4)_2 \cdot \text{H}_2\text{O}$. One can see that the greater the content of monocalcium phosphate monohydrate $\text{Ca}(\text{H}_2\text{PO}_4)_2 \cdot \text{H}_2\text{O}$ in powder mixture, the more noticeable its main reflex at normalized graphs. Chemical reaction (2) of brushite dehydration taking place during disaggregation in acetone medium in powder mixture “Pyro” is presented below.



TA data of powder mixtures “Pyro” ($\text{Ca}/\text{P} = 1$) and “Pyro_10Poly” ($\text{Ca}/\text{P} = 0.95$) prepared in mechanical activation conditions in aqua medium from calcium lactate pentahydrate $\text{Ca}(\text{C}_3\text{H}_5\text{O}_3)_2 \cdot 5\text{H}_2\text{O}$ and monocalcium phosphate monohydrate $\text{Ca}(\text{H}_2\text{PO}_4)_2 \cdot \text{H}_2\text{O}$, disaggregated in acetone medium, and TA of starting components (calcium lactate pentahydrate $\text{Ca}(\text{C}_3\text{H}_5\text{O}_3)_2 \cdot 5\text{H}_2\text{O}$ and monocalcium phosphate monohydrate $\text{Ca}(\text{H}_2\text{PO}_4)_2 \cdot \text{H}_2\text{O}$) are presented in Figure 3. Total mass loss for powder mixtures “Pyro” ($\text{Ca}/\text{P} = 1$) was 40%. Total mass loss for powder mixtures “Pyro_10Poly” ($\text{Ca}/\text{P} = 0.95$) was 39%. All processes provided mass loss of the powder mixtures under investigation during heating finished up to 500 °C. As we can assume according to data of XRD analysis of powder mixtures after treatment in acetone medium and the accordant reaction (1), composition of powder mixtures included monetite, lactic acid, and starting components (calcium lactate pentahydrate $\text{Ca}(\text{C}_3\text{H}_5\text{O}_3)_2 \cdot 5\text{H}_2\text{O}$ and monocalcium phosphate monohydrate $\text{Ca}(\text{H}_2\text{PO}_4)_2 \cdot \text{H}_2\text{O}$).

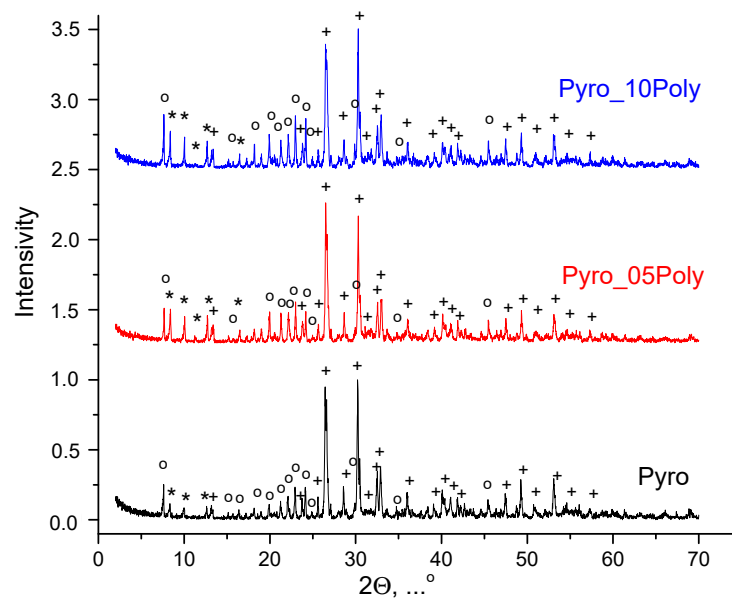


Figure 2. XRD data for powder mixtures prepared in mechanical activation conditions from calcium lactate pentahydrate $\text{Ca}(\text{C}_3\text{H}_5\text{O}_3)_2 \cdot 5\text{H}_2\text{O}$ and monocalcium phosphate monohydrate $\text{Ca}(\text{H}_2\text{PO}_4)_2 \cdot \text{H}_2\text{O}$ after disaggregation in acetone medium: *— $\text{Ca}(\text{C}_3\text{H}_5\text{O}_3)_2 \cdot 5\text{H}_2\text{O}$ (according scientific literature data [49–51]); o— $\text{Ca}(\text{H}_2\text{PO}_4)_2 \cdot \text{H}_2\text{O}$ (PDF card 9-347); +— CaHPO_4 (PDF card 9-80).

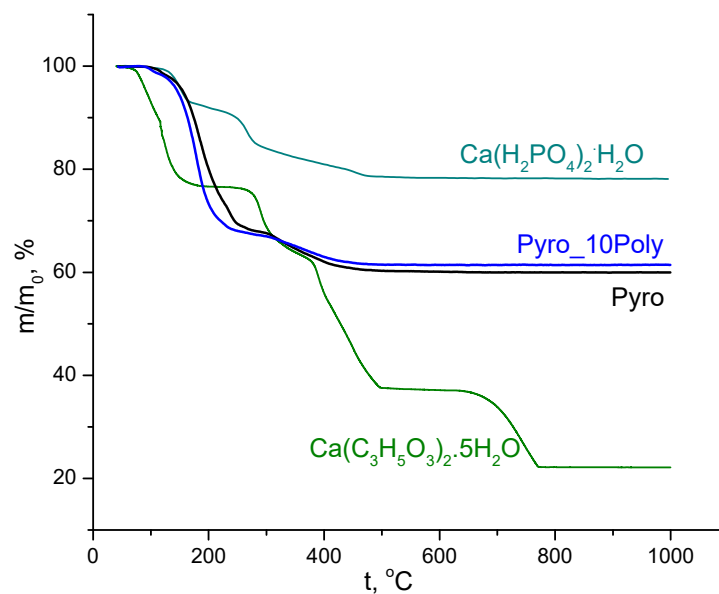
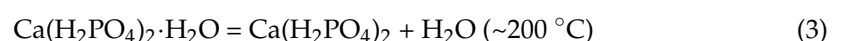
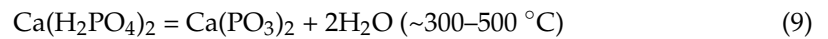
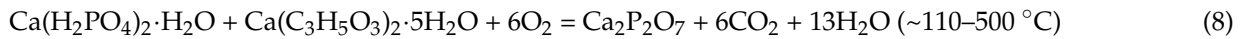
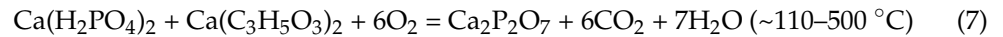
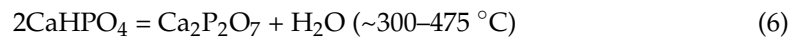
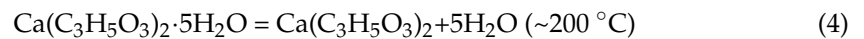


Figure 3. TA of powder mixtures “Pyro” ($\text{Ca}/\text{P} = 1$) and “Pyro_10Poly” ($\text{Ca}/\text{P} = 0.95$) prepared in mechanical activation conditions from calcium lactate pentahydrate $\text{Ca}(\text{C}_3\text{H}_5\text{O}_3)_2 \cdot 5\text{H}_2\text{O}$ and disaggregated in acetone medium; TA of starting components (calcium lactate pentahydrate $\text{Ca}(\text{C}_3\text{H}_5\text{O}_3)_2 \cdot 5\text{H}_2\text{O}$ and monocalcium phosphate monohydrate $\text{Ca}(\text{H}_2\text{PO}_4)_2 \cdot \text{H}_2\text{O}$).

So, we can suggest the following reactions that can take place during heating: dehydration of hydrated salts (reactions (3) and (4) [10,52]), decomposition of lactic acid (reaction (5) [53]), formation of calcium pyrophosphate via condensation (6) [10], synthesis of calcium pyrophosphate due to interaction of monocalcium phosphate with calcium lactate (reaction (7)) or due to interaction of monocalcium phosphate monohydrate with calcium lactate pentahydrate (reaction (8)), and formation of calcium polyphosphate due to condensation (reaction (9) [10]).





The form of curves $m/m_0 = f(t)$ in Figure 3 of powder mixtures under investigation are very smooth and differ from curves of starting salts. The smoothness of the lines indicates the possibility of overlapping temperature intervals for listed reactions and their simultaneous occurrence. This difference confirms the possibility both of reactions of condensation (reactions (6) and (9)) and the possibility of formation of calcium pyrophosphate from starting components preserved during treatments in mechanical activation conditions. Differentiation of curves $m/m_0 = f(t)$ for powder mixtures under investigation allows finding several temperatures with maximum mass loss rate. There are 130 °C, 180 °C (the biggest), 240 °C, 320 °C, and 400 °C for powder mixture “Pyro” and 100 °C, 180 °C (the biggest), 230 °C, and 360 °C for powder mixture “Pyro_10Poly”. Mass loss due to CO₂ ($m/Z = 44$) evolving took place in interval 110–500 °C with a maximum of 190 °C. Mass loss due to H₂O ($m/Z = 18$) evolving took place in three intervals: 80–130 °C (with the maximum at 105 °C), 130–260 °C (with the maximum at 190 °C), 290–500 °C (with wide maximum 330–400 °C).

XRD data for powder mixtures prepared in mechanical activation conditions from calcium lactate pentahydrate $\text{Ca}(\text{C}_3\text{H}_5\text{O}_3)_2 \cdot 5\text{H}_2\text{O}$ and monocalcium phosphate monohydrate $\text{Ca}(\text{H}_2\text{PO}_4)_2 \cdot \text{H}_2\text{O}$, disaggregated in acetone medium, after heat treatment at 600 °C is presented in Figure 4. The phase composition of prepared powders “Pyro”, “Pyro_05Poly”, “Pyro_10Poly” after heat treatment at 600 °C was presented by γ -calcium pyrophosphate $\gamma\text{-Ca}_2\text{P}_2\text{O}_7$.

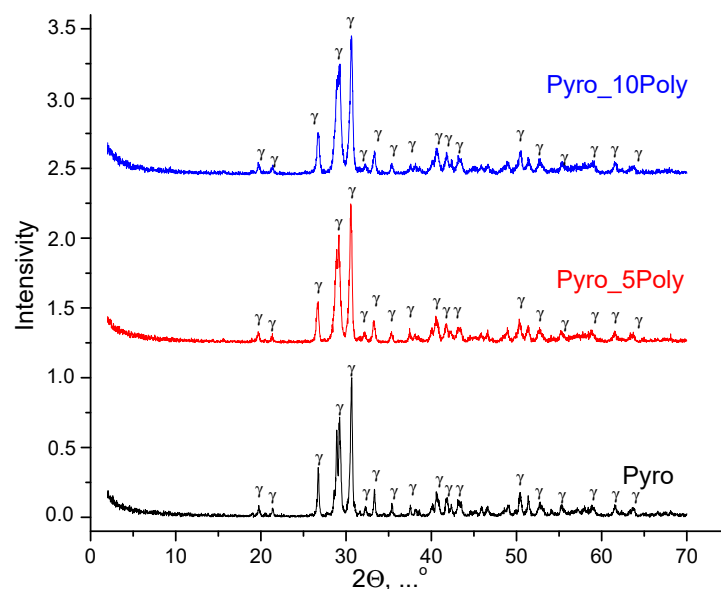
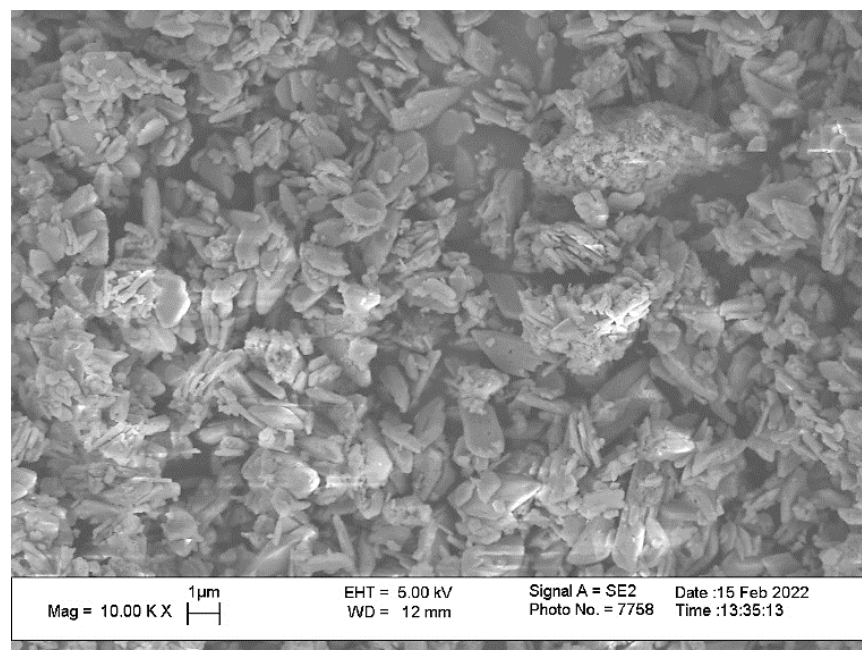
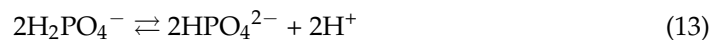
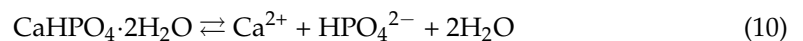


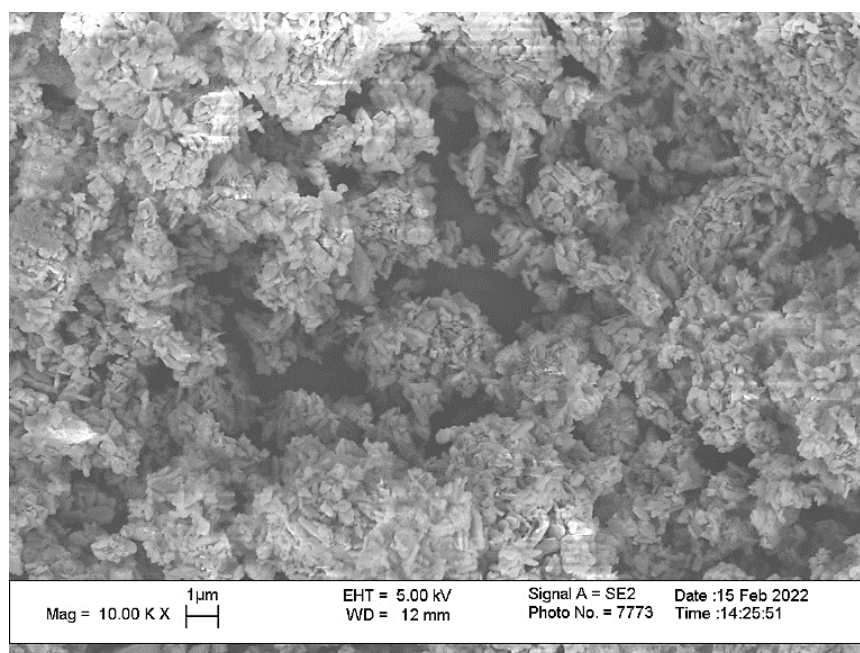
Figure 4. XRD data for powder mixtures prepared in mechanical activation conditions from calcium lactate pentahydrate $\text{Ca}(\text{C}_3\text{H}_5\text{O}_3)_2 \cdot 5\text{H}_2\text{O}$ and monocalcium phosphate monohydrate $\text{Ca}(\text{H}_2\text{PO}_4)_2 \cdot \text{H}_2\text{O}$, disaggregated in acetone medium, after heat treatment at 600 °C: $\gamma\text{-}\gamma\text{-Ca}_2\text{P}_2\text{O}_7$ (PDF card 17-499).

SEM images of powders “Pyro”, “Pyro_05Poly”, “Pyro_10Poly” after heat treatment at 600 °C are presented in Figure 5. One can see that particles of powders are fine and the dimension of particles is dependent on the preset molar ratio of powders. Particles have a platelike morphology. Particles after heat treatment indeed inherit the shape of the particles after synthesis and drying. The lower the molar ratio Ca/P, the smaller the dimensions of particles are. The dimensions of particles of powder “Pyro” are in the interval 0.2–2 µm. The dimensions of particles of powder “Pyro_05Poly” are in interval 0.1–1 µm. The dimensions of particles of powder “Pyro_10Poly” are in the interval 0.1–0.5 µm. One of the reasons for fine particle formation consisted in using synthesis in the mechanical activation conditions. The advantages of using mechanical activation conditions were shown for monetite CaHPO_4 synthesis before [10]. Presence of the lactic acid that acted as a surfactant [44] in suspensions during synthesis in mechanical activation conditions and during drying can be accepted as additional reason of fine particles formation. According to XRD analysis, brushite, the metastable dicalcium phosphate dihydrate $\text{CaHPO}_4 \cdot 2\text{H}_2\text{O}$ was detected only in the phase composition of the powder “Pyro”. Powders “Pyro_05Poly” and “Pyro_10Poly” contained monetite CaHPO_4 . All prepared powders after mechanical activation of starting components in water contained monocalcium phosphate monohydrate $\text{Ca}(\text{H}_2\text{PO}_4)_2 \cdot \text{H}_2\text{O}$. As all these calcium phosphates are slightly soluble in water to varying degrees, the following processes (reaction (10)–(13)) could take place during a week of drying of aqueous suspensions providing mass transfer between the particles of calcium phosphate phases.

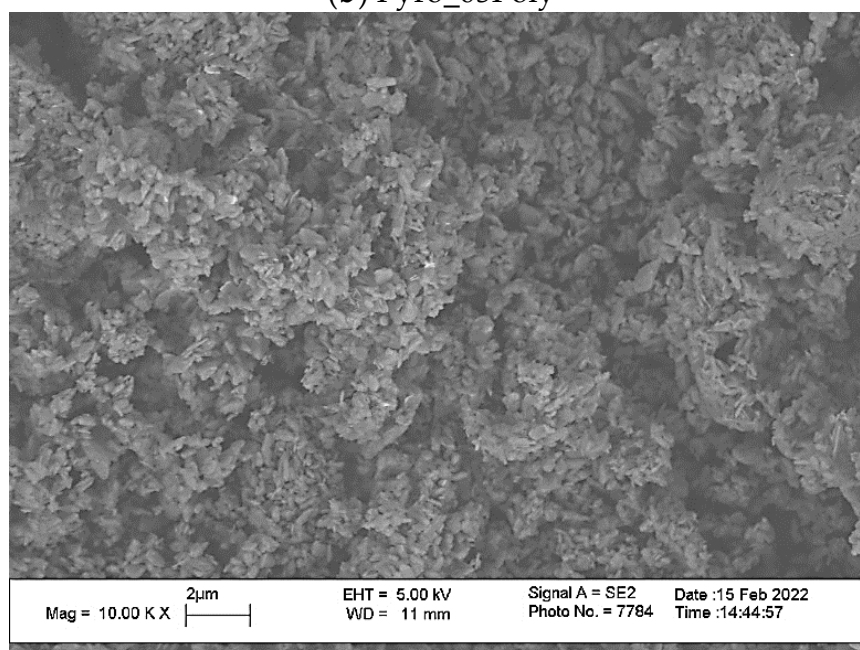


(a) Pyro

Figure 5. Cont.



(b) Pyro_05Poly



(c) Pyro_10Poly

Figure 5. Micro photos of powders after heat treatment at 600 °C: “Pyro” (a); “Pyro_05Poly” (b); “Pyro_10Poly” (c).

Brushite $\text{CaHPO}_4 \cdot 2\text{H}_2\text{O}$ ($pK_{sp} = 6.59$) is a more soluble salt than monetite CaHPO_4 ($pK_{sp} = 6.90$), and monocalcium phosphate monohydrate $\text{Ca}(\text{H}_2\text{PO}_4)_2 \cdot \text{H}_2\text{O}$ ($pK_{sp} = 1.14$) is significantly more soluble than brushite $\text{CaHPO}_4 \cdot 2\text{H}_2\text{O}$ and monetite CaHPO_4 [2]. So, processes of dissolution/crystallization in suspension “Pyro” led to an increase in the particle size of brushite $\text{CaHPO}_4 \cdot 2\text{H}_2\text{O}$ during transformation of suspension to the powder. The lower the molar ratio of Ca/P in the powders from “Pyro” to “Pyro_10Poly”, the bigger the quantity of monocalcium phosphate monohydrate $\text{Ca}(\text{H}_2\text{PO}_4)_2 \cdot \text{H}_2\text{O}$ in the water suspensions was. Therefore, the lower the preset molar ratio of Ca/P in samples under investigation, the greater the concentration of HPO_4^{2-} and 2H^+ ions in an aqueous solution surrounding calcium phosphate particles of suspensions were.

The bigger quantity of HPO_4^{2-} and 2H^+ ions in suspensions “Pyro_05Poly” and “Pyro_10Poly” could shift the equilibrium in reactions (10) and (11) to the left. This shift thereby reduced the recrystallization rate of solid phase particles of monetite CaHPO_4 . So, the possibility of dissolution/crystallization in suspension “Pyro” was more likely than in suspensions “Pyro_05Poly” and “Pyro_10Poly”. For this reason, the composition of prepared suspensions and the phenomenon of inheritance of synthesized particle morphology can explain the decrease in particle size in heat treated at $600\text{ }^\circ\text{C}$ powders with a decrease in preset Ca/P molar ratio from 1 to 0.95. Reactions with fast, big volumes evolving of gaseous phase during heat treatment of powders could be the additional reason for fine powder formation. It should be noted that small particles of all powders are collected in aggregates. Particle size distribution of powder prepared in mechanical activation conditions from calcium lactate pentahydrate $\text{Ca}(\text{C}_3\text{H}_5\text{O}_3)_2 \cdot 5\text{H}_2\text{O}$ and monocalcium phosphate monohydrate $\text{Ca}(\text{H}_2\text{PO}_4)_2 \cdot \text{H}_2\text{O}$, disaggregated in acetone medium, after heat treatment at $600\text{ }^\circ\text{C}$ is presented in Figure 6. The size of most occurring aggregates of particles for powder “Pyro” estimated as $5.0\text{ }\mu\text{m}$, for powder “Pyro_05Poly”- $12.1\text{ }\mu\text{m}$ and for powder “Pyro_10Poly”- $12.5\text{ }\mu\text{m}$.

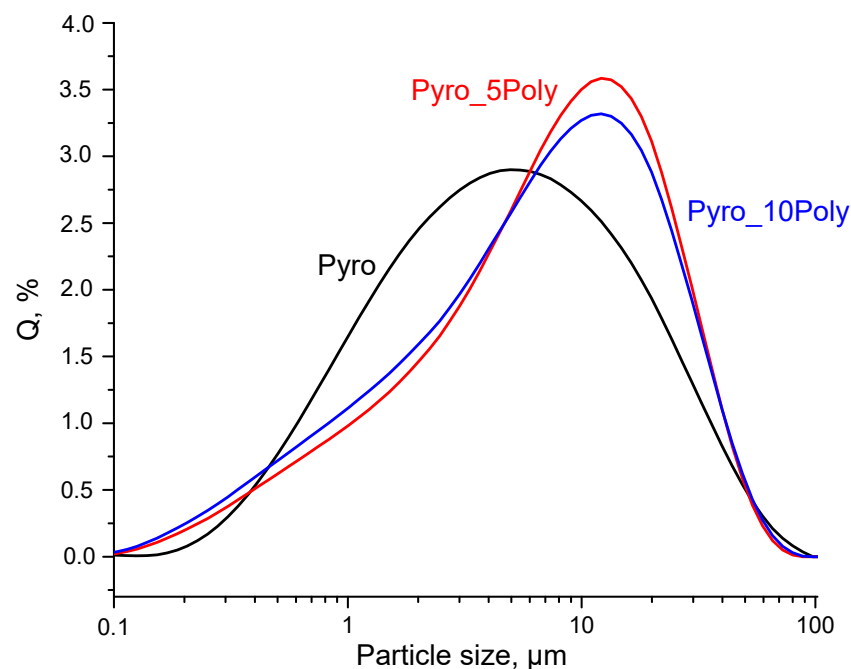


Figure 6. Particle size distribution of powders prepared in mechanical activation conditions from calcium lactate pentahydrate $\text{Ca}(\text{C}_3\text{H}_5\text{O}_3)_2 \cdot 5\text{H}_2\text{O}$ and monocalcium phosphate monohydrate $\text{Ca}(\text{H}_2\text{PO}_4)_2 \cdot \text{H}_2\text{O}$, disaggregated in acetone medium, after heat treatment at $600\text{ }^\circ\text{C}$.

According to XRD data for ceramic samples based on powders “Pyro”, “Pyro_05Poly” and “Pyro_10Poly” fired at $900\text{ }^\circ\text{C}$, $1000\text{ }^\circ\text{C}$, and $1100\text{ }^\circ\text{C}$, the phase composition of all samples was presented by β -calcium pyrophosphate $\beta\text{-Ca}_2\text{P}_2\text{O}_7$. XRD data for ceramic samples “Pyro”, “Pyro_05Poly”, “Pyro_10Poly” after firing at $900\text{ }^\circ\text{C}$, $1000\text{ }^\circ\text{C}$ and $1100\text{ }^\circ\text{C}$ are presented in Supplementary Materials at XRD data for ceramic samples after firing at $1100\text{ }^\circ\text{C}$ are presented in Figure 7. So, we can conclude that presence of calcium polyphosphate $\text{Ca}(\text{PO}_3)_2$ up to 10 mol% introduced via excess of monocalcium phosphate monohydrate $\text{Ca}(\text{H}_2\text{PO}_4)_2 \cdot \text{H}_2\text{O}$ cannot be detected using XRD analysis.

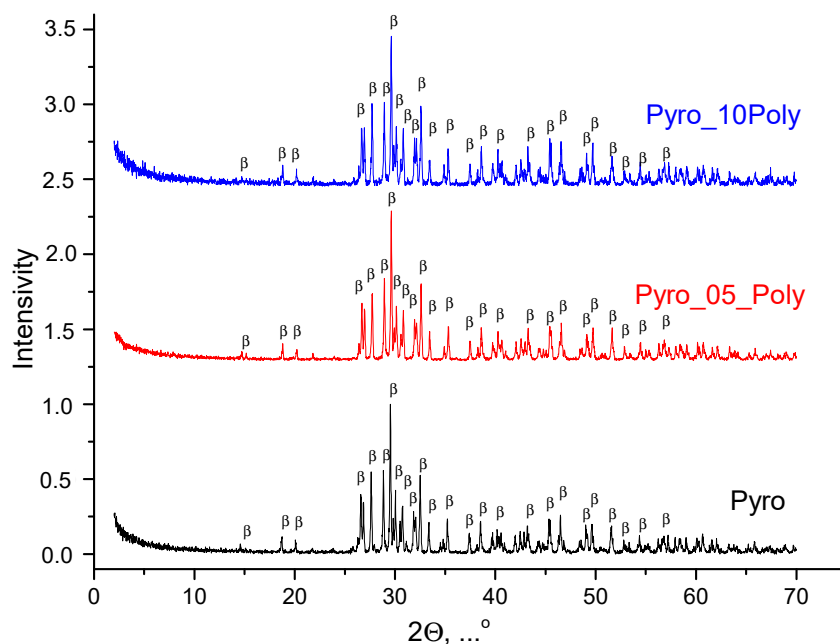


Figure 7. XRD data for ceramic samples “Pyro”, “Pyro_05Poly”, and “Pyro_10Poly” fired at 1100 °C: β—β-Ca₂P₂O₇ (PDF card 9-346).

At the same time, Figure 8 (“Pyro”), Figure 9 (“Pyro_05Poly”), and Figure 10 (“Pyro_10Poly”) present SEM micrographs of surface and cross-section of samples, allowing us to conclude the obvious influence of firing temperature and quantity of sintering additive on the microstructure of ceramics.

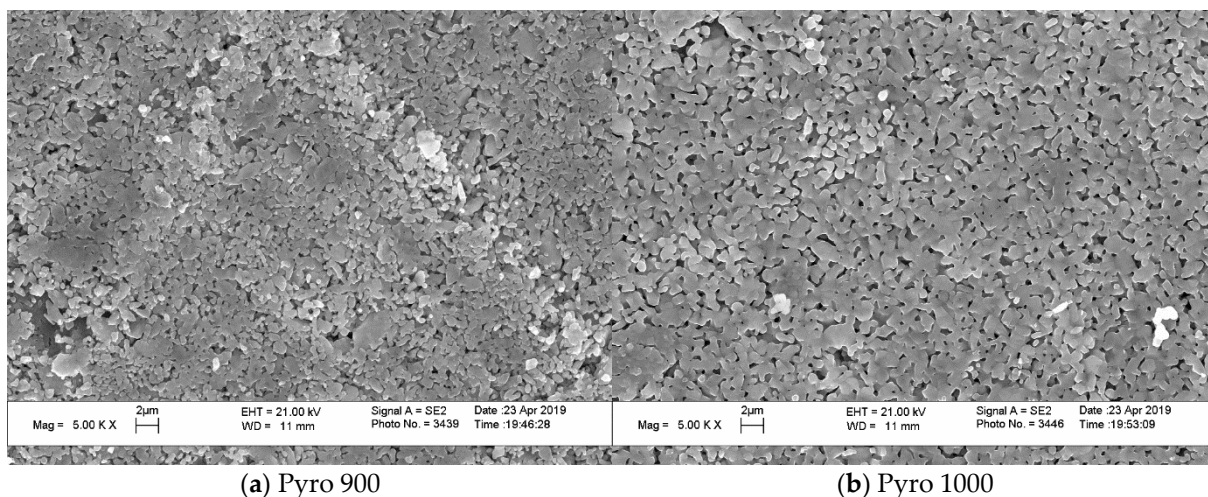
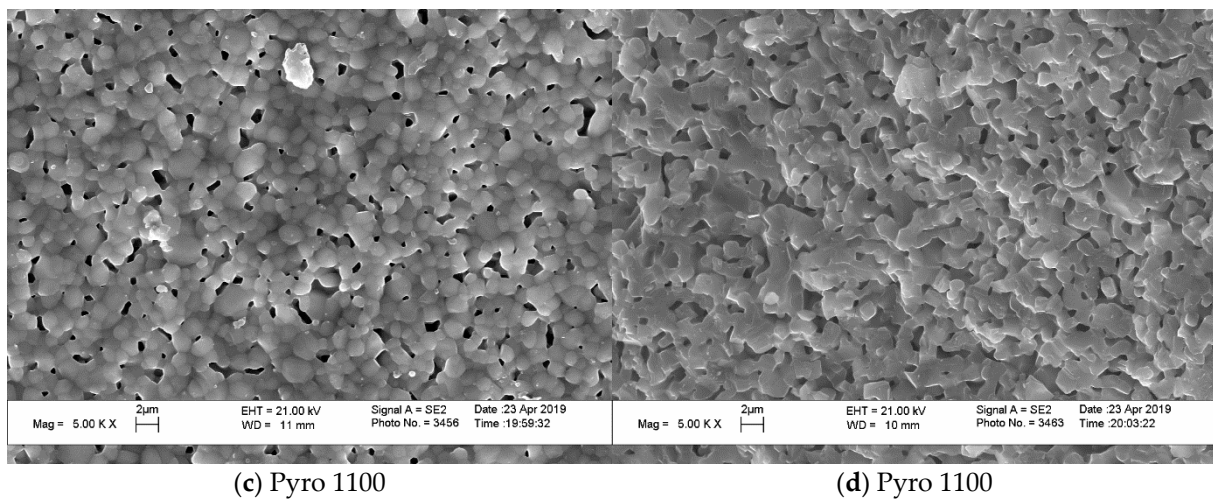


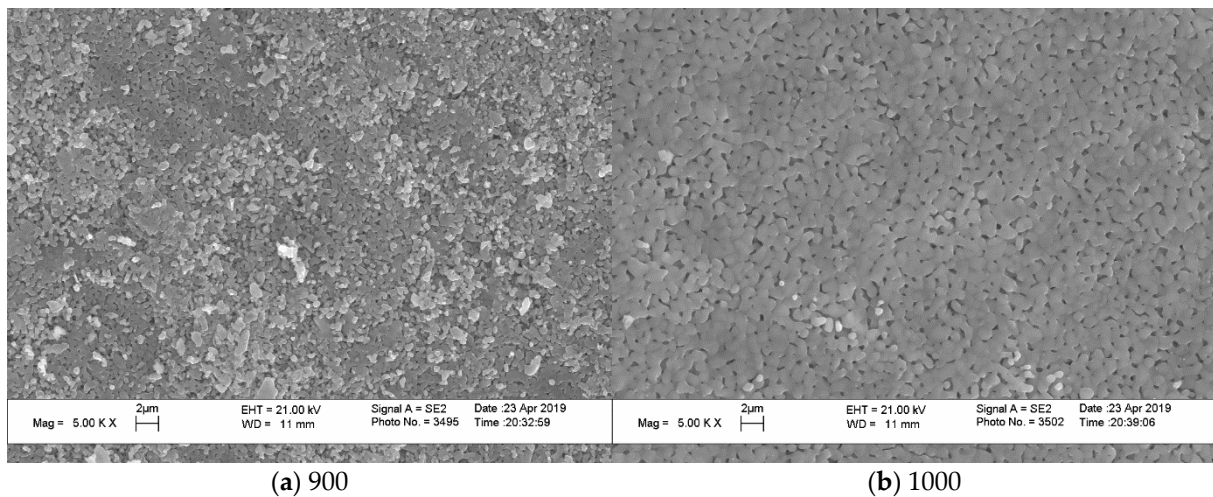
Figure 8. Cont.



(c) Pyro 1100

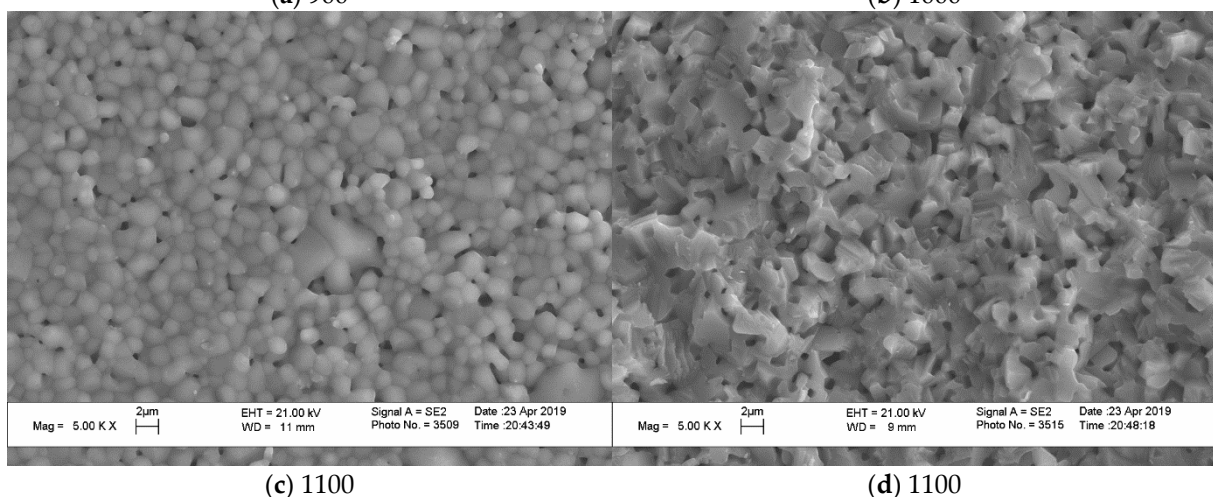
(d) Pyro 1100

Figure 8. SEM micrographs of surface (a–c) and cross-section (d) of ceramic samples “Pyro” fired at 900 °C (a), 1000 °C (b), and 1100 °C (c,d).



(a) 900

(b) 1000



(c) 1100

(d) 1100

Figure 9. SEM micrographs of surface (a–c) and cross section (d) of ceramic samples “Pyro_05Poly” fired at 900 °C (a), 1000 °C (b) and 1100 °C (c,d).

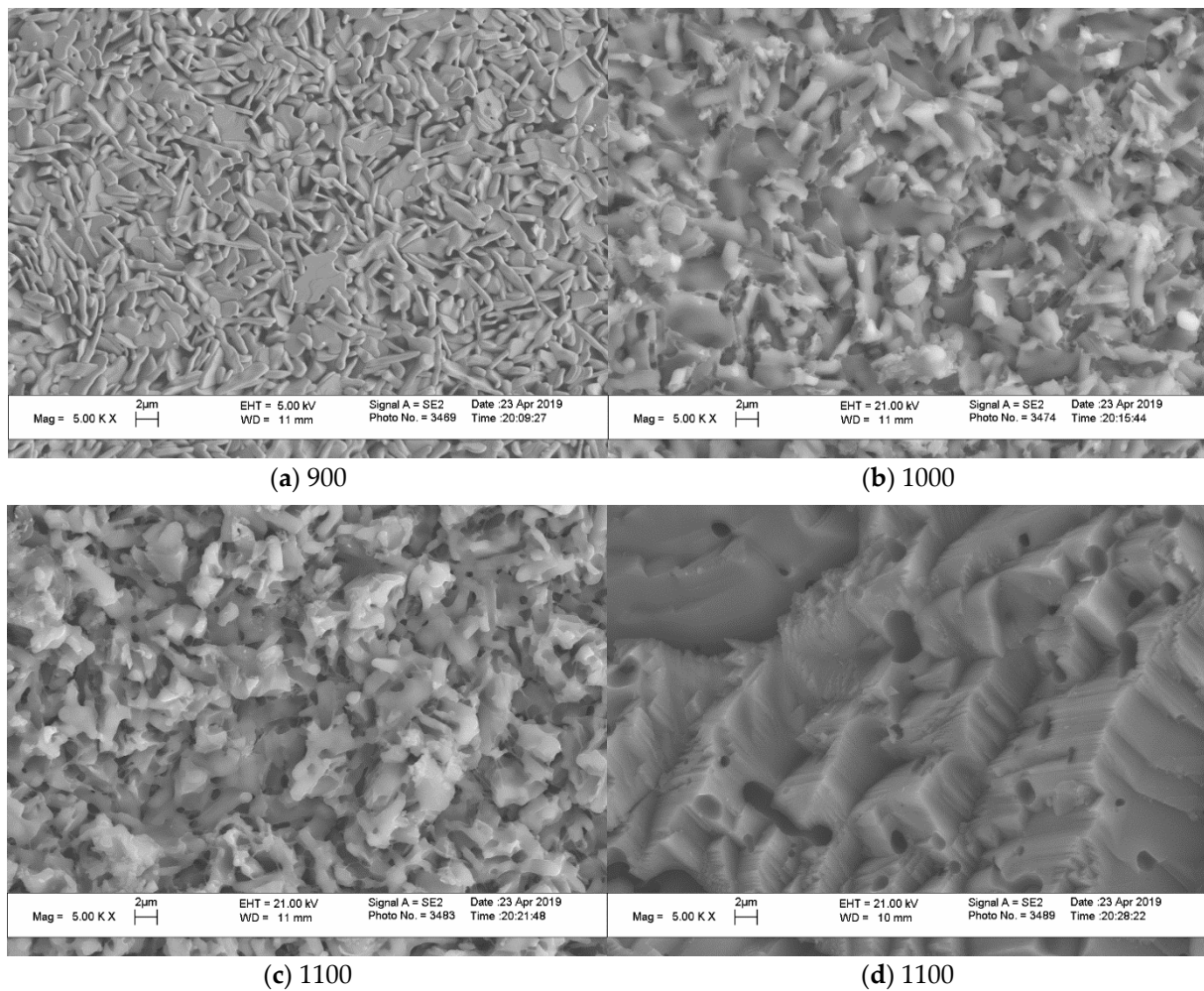


Figure 10. SEM micrographs of surface (a–c) and cross section (d) of ceramic samples “Pyro_10Poly” fired at 900 °C (a), 1000 °C (b), and 1100 °C (c,d).

The grain size of ceramics increased both with the growth in firing temperature and with decreasing Ca/P molar ratio of powder mixtures. The grain size of ceramic samples based on powder “Pyro” (Figure 8) increased from 1 μm after firing at 900 °C (Figure 8a) to 2 μm after firing at 1100 °C (Figure 8c,d). It should be noted that impressions from the microstructure of surface and microstructure of cross-section after firing at 1100 °C are very much similar.

The grain size of ceramic samples based on powder “Pyro_05Poly” (Figure 9) increased from ~0.5–1 μm after firing at 900 °C (Figure 9a) to ~2 μm after firing at 1100 °C (Figure 9c,d). It should be noted that the sample despite the same development in grain size as it was for ceramics based on powder “Pyro” looks sintered to a greater extent. Microstructure of cross-section of the ceramic sample after firing at 1100 °C (Figure 9d) give us the opportunity to conclude that it formed at the presence of liquid phase. Temperatures of firing 1000 and 1100 °C are higher than eutectic temperature (970 °C) in the CaO-P₂O₅ system according to literature data [16]. So, the presence of calcium polyphosphate Ca(PO₃)₂ with the preset quantity of 5 mol.% creates the conditions for liquid phase sintering in ceramics based on powder “Pyro_05Poly”.

The microstructure of ceramics based on powder “Pyro_10Poly” (Figure 10) demonstrates the influence of additive provoking liquid phase sintering. One can see grains with dimensions 1–4 μm on the surface of the ceramic sample after firing at 900 °C (Figure 10a). Some grains have an elongated form. After firing at 1000 °C (Figure 10b), grains on the surface of the ceramic sample based on powder “Pyro_10Poly” have dimensions 2–4 μm;

after firing at 1100 °C on the surface, one can see grains 2–4 μm (Figure 10c). Images of surfaces of ceramic samples based on powder “Pyro_10Poly” after firing at 1000 °C and 1100 °C give us an opportunity to suppose that grains grew up in the direction above the surface. These phenomena were quite possible because the firing temperature 1000 °C and 1100 °C were higher than both the melting point (~984 °C) of calcium polyphosphate and eutectic point (~970 °C) in the quasi binary system $\text{Ca}_2\text{P}_2\text{O}_7\text{-Ca}(\text{PO}_3)_2$ [16,54]. It is also well known that vapor pressure of polyphosphate melts is quite high [55]. Micrograph of cross-section (Figure 10d) of ceramics based on powder “Pyro_10Poly” after firing at 1100 °C does not show any grains and determination of their dimensions is not possible. One can see closed pores with dimensions 1–4 μm. The microstructure of cross-section gives us an opportunity to make a conclusion about presence of the melt in the ceramic sample based on powder “Pyro_10Poly” during firing at 1100 °C.

Dependences of relative diameter (D/D_0 , %) and apparent density (ρ , g/cm³) of ceramic samples from firing temperature are presented in Figure 11.

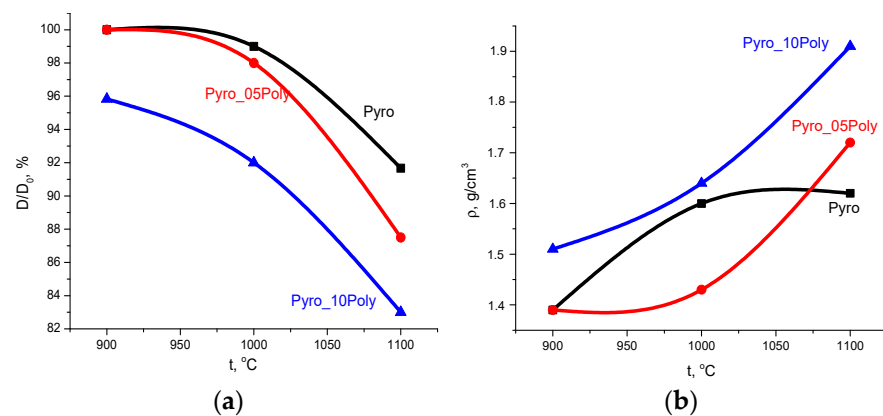


Figure 11. Dependences of relative diameter (a) and an apparent density (b) of ceramic samples from firing temperature.

Linear shrinkage (Figure 11a) increased for all samples with the growth in firing temperature. The maximum linear shrinkage of ceramics based on powder “Pyro” was ~10% after firing at 1100 °C. The maximum linear shrinkage of ceramics based on powder “Pyro_05Poly” was ~13% after firing at 1100 °C. The linear shrinkage of ceramics based on powder “Pyro_10Poly” increased from 4% at 900 °C to 17% at 1100 °C.

Density of ceramic samples (Figure 11b) prepared from the powders “Pyro_05Poly” and “Pyro_10Poly” increased with growth in firing temperature from 1.4 g/cm³ and 1.51 g/cm³ at 900 °C to 1.7 g/cm³ (55%) and 1.9 g/cm³ (60%) at 1100 °C, respectively. The density of ceramic samples based on powders “Pyro” achieved 1.6 g/cm³ (50%) after firing at 1000 °C; after firing at 1100 °C, this value became the same. In comparison with theoretical density of β -calcium pyrophosphate (3.12 g/cm³), we have to admit that as a result, we prepared quite porous ceramic samples from fine powders of γ -calcium pyrophosphate.

The results of the MTT-test are presented in Figure 12. The MTT assay showed the viability assay of NCTC L929 cells in the presence of liquid extracts from ceramic samples under investigation, i.e., “Pyro”, “Pyro_05Poly”, and “Pyro_10Poly” after 48 h cultivation sample and control. The Mann–Whitney U test was performed to assess the significance of the effect of liquid extracts from ceramic samples under investigation i.e., “Pyro”, “Pyro_05Poly”, and “Pyro_10Poly”, on the cell viability assay. There was no significant difference between the groups “Pyro_05 Poly” and “Pyro_10 Poly” when comparing control. The effect of liquid extracts from ceramic samples “Pyro” (*) obtained results is significantly different from the control sample.

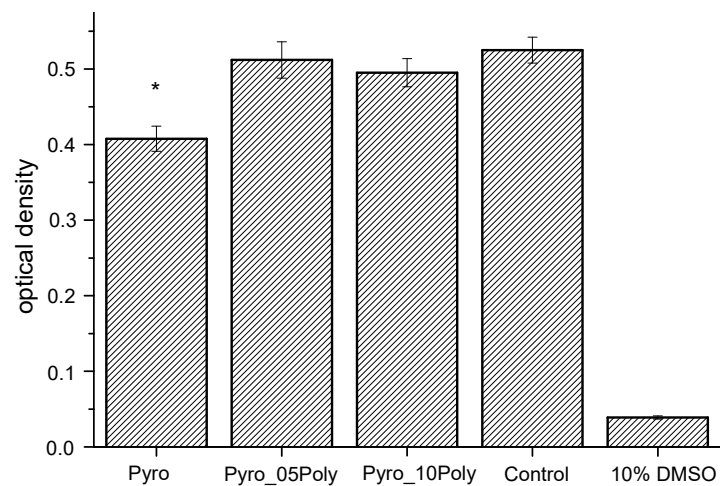


Figure 12. The MTT viability assay of NCTC L929 cells in the presence of liquid extracts from ceramic samples (firing temperature 1100 °C) under investigation, i.e., “Pyro”, “Pyro_05Poly”, “Pyro_10Poly”, control, and 10% DMSO after 48 h cultivation (mean \pm SD, n = 10).

The results of determining the viability of cells cultured on the surface of the studied materials on the second (Figure 13) and on the second and seventh day (Figure 14) confirmed that the proliferative activity of cells was observed on the surface of all the samples studied.

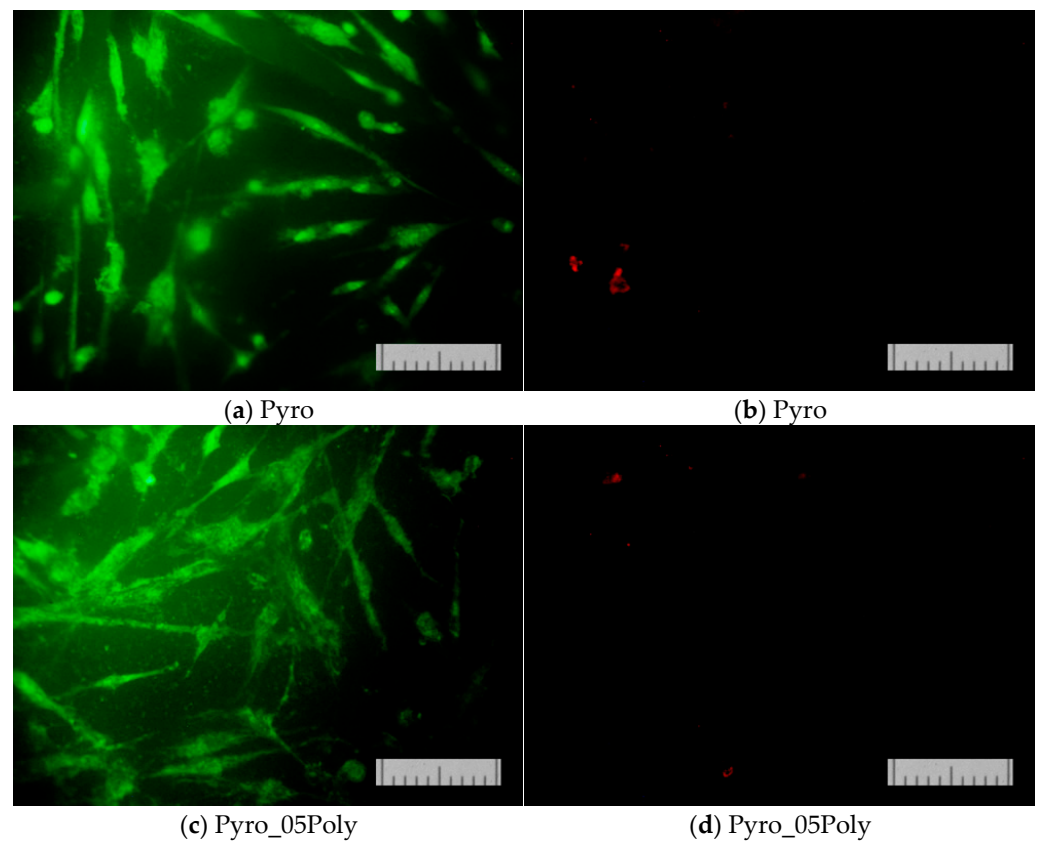


Figure 13. *Cont.*

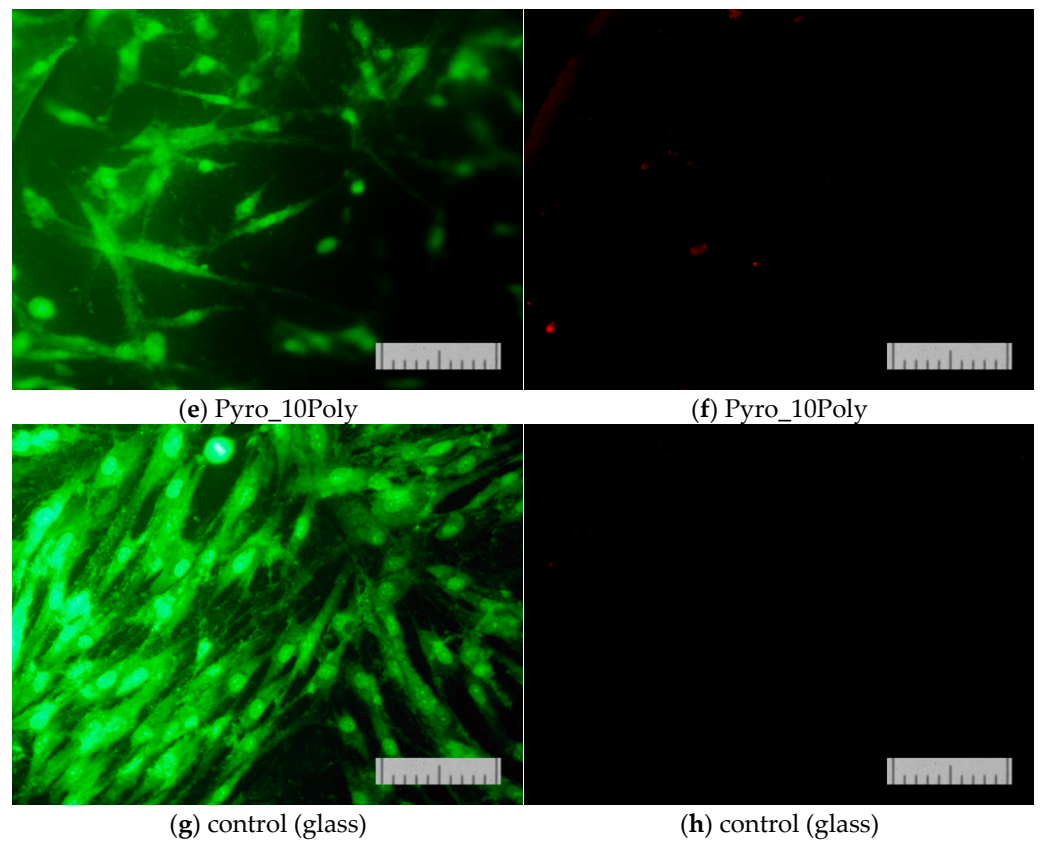


Figure 13. The appearance of the dental pulp stem cells on the surface of ceramic samples (firing temperature 1100 °C) under investigation, i.e., ceramic samples prepared based on powders “Pyro” (a,b), “Pyro_05Poly” (c,d), “Pyro_10Poly” (e,f), and control (g,h) after direct contact procedure for 2 days. Fluorescent staining was made with SYTO 9 (a,c,e,g) and propidium iodide (b,d,f,h). Bar 100 µm.

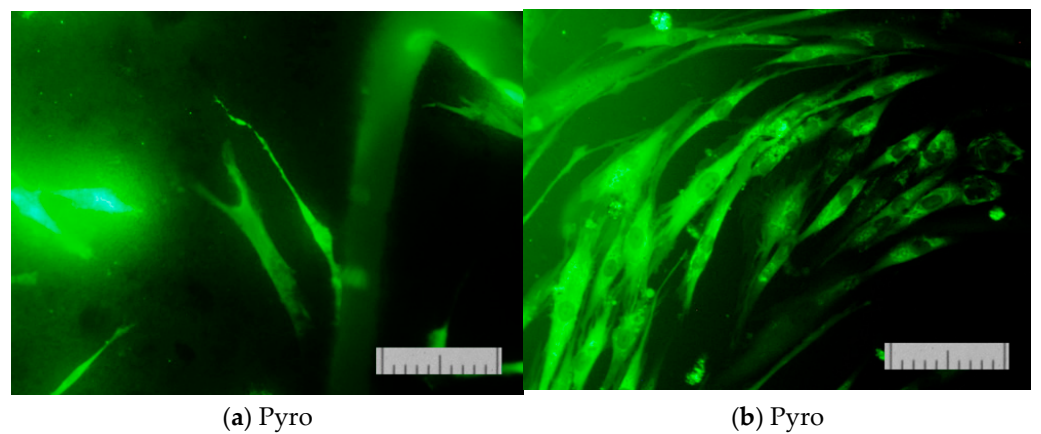


Figure 14. *Cont.*

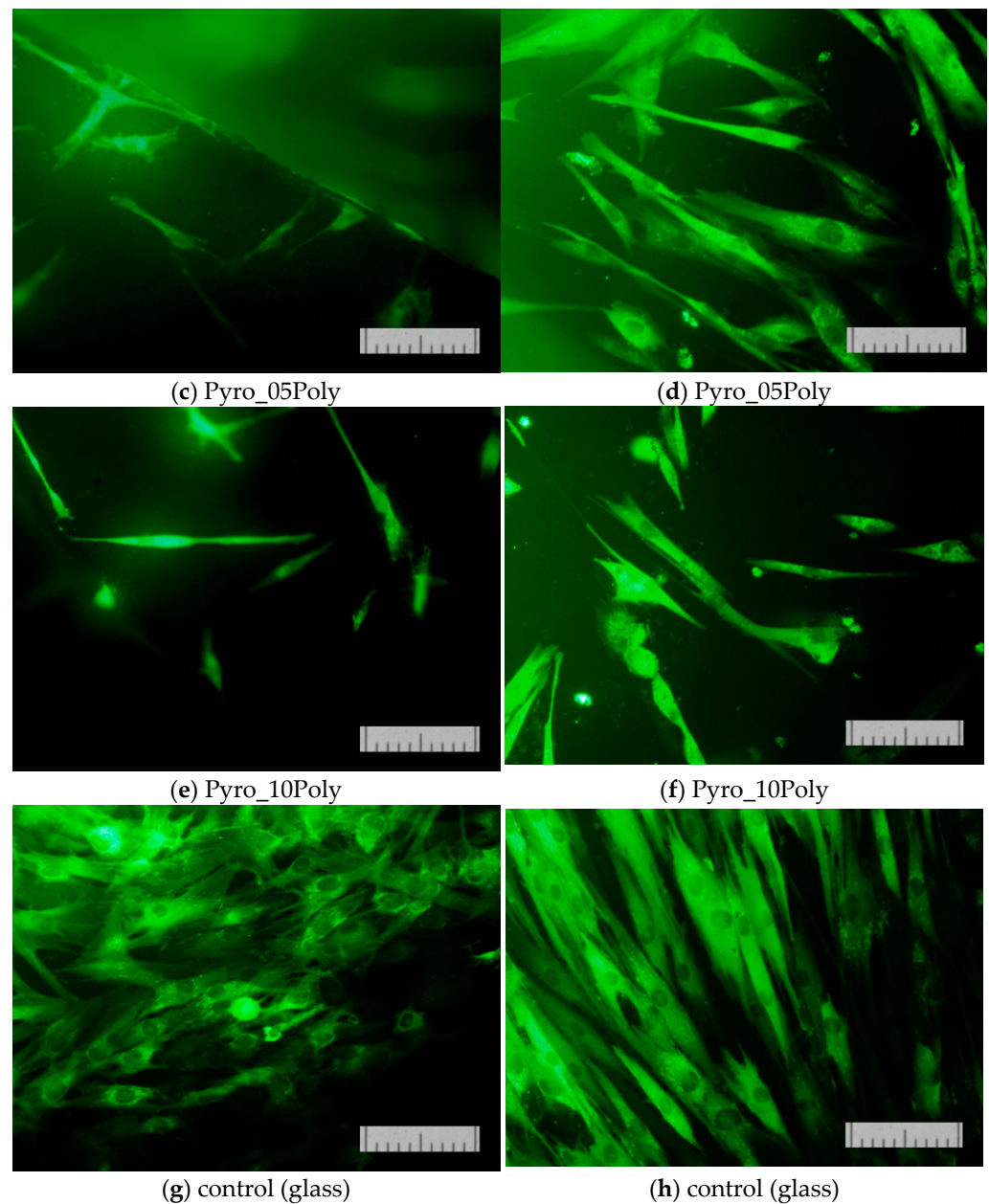
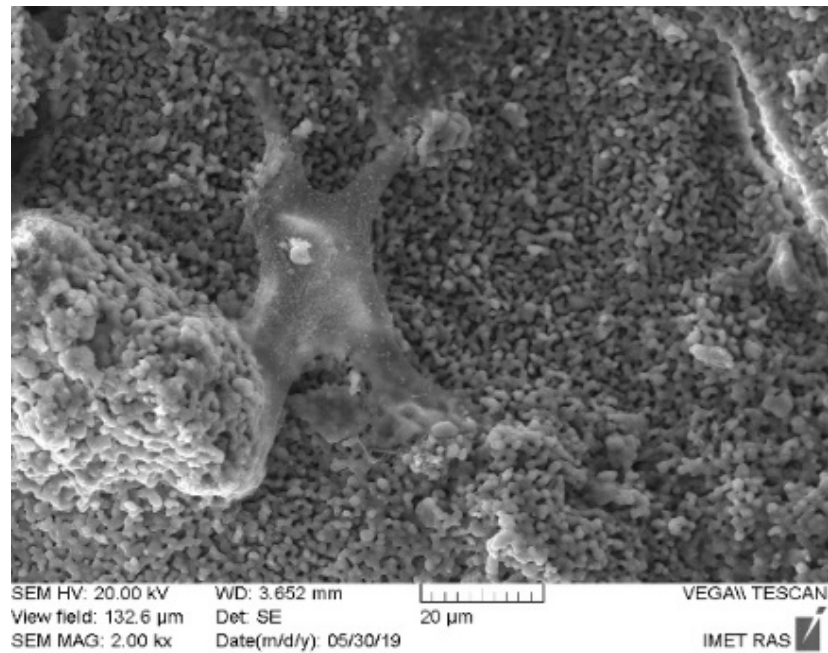


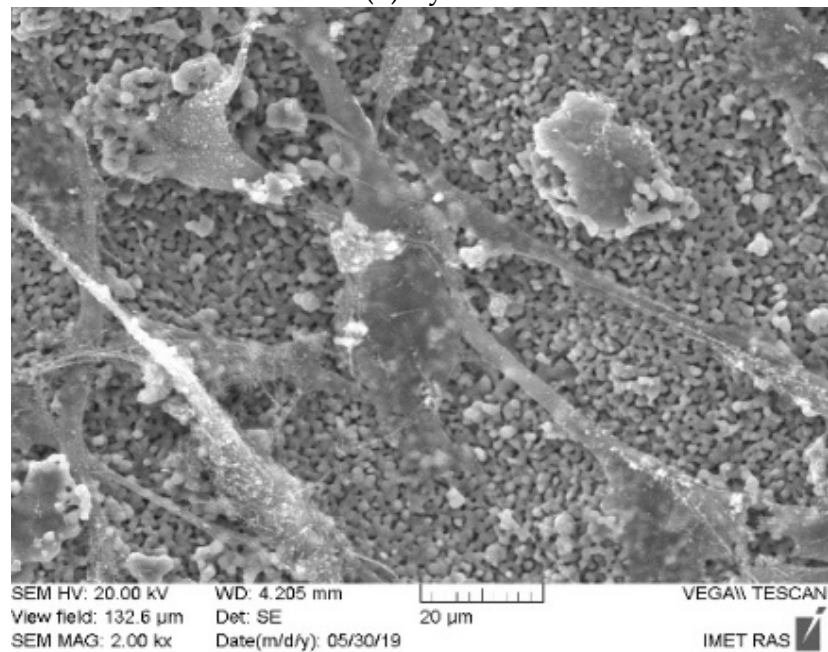
Figure 14. The appearance of the dental pulp stem cells of the surface of ceramic samples (firing temperature 1100 °C) under investigation, i.e., “Pyro” (a,b), “Pyro_05Poly” (c,d), “Pyro_10Poly” (e,f), and control (g,h) after direct contact procedure for 2 (a,c,e,g) and 7 (b,d,f,h) days. Fluorescent staining was made with SYTO 9. Bar—100 μ m.

Normal morphology of DPSC 32 cells is observed on all the studied samples. However, the density of the cell layer on the surface of the studied samples after cultivation for two or seven days was slightly lower than in the control (on the cover glass). This phenomenon was apparently due to the conditions of initial cell adhesion. Nevertheless, the absence of dead cells whose nuclei are stained with propidium iodide indicates the absence of cytotoxic effects of the ceramic materials prepared based on powders “Pyro”, “Pyro_05Poly”, and “Pyro_10Poly”. The density of the cell layer on the surface of the studied samples after cultivation for seven days (Figure 14b,d,f) demonstrate the slight dependence from preset Ca/P molar ratios in starting powders and ceramic samples. The lower the Ca/P molar ratio, the lower the density of cell layer. This phenomenon can be explained with the more acidic nature of ceramic samples (“Pyro_05Poly”, “Pyro_10Poly”) containing the calcium polyphosphate phase in a very slight quantity not detected by XRD analysis.

Figure 15 presents micrographs of cells fixed to the ceramic surface after cultivation for two days.



(a) Pyro



(b) Pyro_05Poly

Figure 15. Cont.

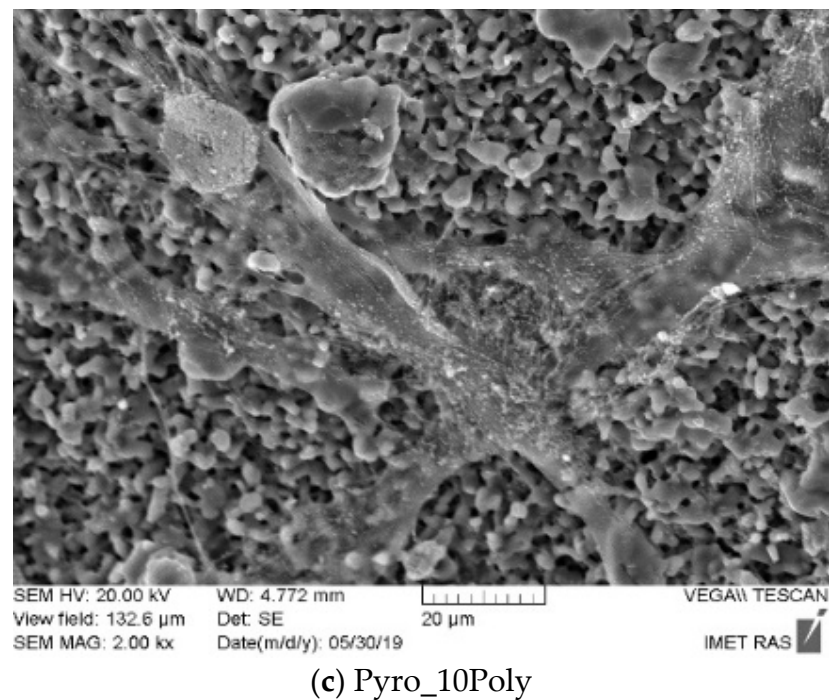


Figure 15. SEM images of cells on the surface of ceramic samples (firing temperature 1100 °C) under investigation, i.e., “Pyro” (a), “Pyro_05Poly” (b), “Pyro_10Poly” (c) after 2 days of cultivation.

These images (Figure 15) demonstrate the good adhesion of cells on the surface of β -calcium pyrophosphate β -Ca₂P₂O₇ ceramic samples prepared based on powders “Pyro” (a), “Pyro_05Poly” (b), and “Pyro_10Poly” (c).

Data from *in vitro* biological experiments confirmed the biocompatibility of the obtained β -calcium pyrophosphate β -Ca₂P₂O₇ ceramic materials and their ability to support cells proliferation.

4. Conclusions

The original method of γ -calcium pyrophosphate γ -Ca₂P₂O₇ powder preparation was used. To prepare powders of γ -calcium pyrophosphate γ -Ca₂P₂O₇ with preset molar ratios Ca/P = 1, 0.975, and 0.95 powder mixtures based on calcium lactate pentahydrate Ca(C₃H₅O₃)₂·5H₂O and monocalcium phosphate monohydrate Ca(H₂PO₄)₂·H₂O were treated in an aqua medium in mechanical activation conditions, dried, disaggregated in acetone, and heat-treated at 600 °C. The addition of more excess of monocalcium phosphate monohydrate Ca(H₂PO₄)₂·H₂O (with appropriate molar ratio of Ca/P = 1) to the mixture of starting components resulted in lower dimensions of γ -calcium pyrophosphate γ -Ca₂P₂O₇ individual particles. Porous ceramic samples with the relative density of 50% (“Pyro”), 55% (“Pyro_05Poly”), and 60% (“Pyro_10Poly”) in the CaO-P₂O₅ system were created from prepared powders after firing at 1100 °C. The grain size of ceramic samples increased both with the growth in firing temperature and with decreasing molar ratio Ca/P of powder mixtures. Calcium polyphosphate (*t*_{melt} = 984 °C), which formed from monocalcium phosphate monohydrate Ca(H₂PO₄)₂·H₂O, acted similar to a liquid phase sintering additive. It was confirmed by tests *in vitro*, that prepared ceramic materials with preset molar ratios Ca/P = 1, 0.975, and 0.95 and phase composition presented by β -calcium pyrophosphate β -Ca₂P₂O₇ were biocompatible and could maintain bone cells proliferation.

Supplementary Materials: The following supporting information can be downloaded at: <https://www.mdpi.com/article/10.3390/ma15093105/s1>. Figure S1: (XRD data for ceramic samples “Pyro” fired at 900 °C, 1000 °C and 1100 °C: β — β -Ca₂P₂O₇ (PDF card 9-346)); Figure S2: (XRD data for ceramic samples “Pyro_05Poly” fired at 900 °C, 1000 °C and 1100 °C: β — β -Ca₂P₂O₇ (PDF card 9-346)); Figure S3: (XRD data for ceramic samples “Pyro_10Poly” fired at 900 °C, 1000 °C, and 1100 °C: β — β -Ca₂P₂O₇ (PDF card 9-346)).

Author Contributions: Conceptualization, T.S. (Tatiana Safronova); methodology, T.S. (Tatiana Safronova); investigation, A.K. (Andrey Kiselev), I.S., T.S. (Tatiana Shatalova), Y.L., Y.F., O.T., S.T., O.A., A.K. (Alexander Knotko) and T.S. (Tatiana Safronova); writing—original draft preparation, A.K. (Andrey Kiselev) and T.S. (Tatiana Safronova); writing—review and editing, T.S. (Tatiana Safronova); visualization, A.K. (Andrey Kiselev), I.S., T.S. (Tatiana Shatalova), Y.L., Y.F., O.T., S.T., O.A., A.K. (Alexander Knotko) and T.S. (Tatiana Safronova); supervision, T.S. (Tatiana Safronova); project administration, T.S. (Tatiana Safronova); funding acquisition, T.S. (Tatiana Safronova). All authors have read and agreed to the published version of the manuscript.

Funding: This research was funded by Russian Foundation for Basic Research, grant number 18-29-11079.

Institutional Review Board Statement: Not applicable.

Informed Consent Statement: Not applicable.

Data Availability Statement: Not applicable.

Acknowledgments: The research was carried out using the equipment of MSU Shared Research Equipment Center “Technologies for obtaining new nanostructured materials and their complex study” and purchased by MSU in the frame of the Equipment Renovation Program (National Project “Science”) and in the frame of the MSU Program of Development.

Conflicts of Interest: The authors declare no conflict of interest.

References

1. Canillas, M.; Pena, P.; De Aza, A.H.; Rodríguez, M.A. Calcium phosphates for biomedical applications. *Boletín De La Soc. Española De Cerámica Y Vidr.* **2017**, *56*, 91–112. [[CrossRef](#)]
2. Dorozhkin, S.V.; Epple, M. Biological and medical significance of calcium phosphates. *Angew. Chem. Int. Ed.* **2002**, *41*, 3130–3146. [[CrossRef](#)]
3. Pina, S.; Ribeiro, V.P.; Marques, C.F.; Maia, F.R.; Silva, T.H.; Reis, R.L.; Oliveira, J.M. Scaffolding Strategies for Tissue Engineering and Regenerative Medicine Applications. *Materials* **2019**, *12*, 1824. [[CrossRef](#)] [[PubMed](#)]
4. Orlov, N.K.; Putlayev, V.I.; Evdokimov, P.V.; Safronova, T.V.; Klimashina, E.S.; Milkin, P.A. Resorption of Ca_{3-x}M_{2x}(PO₄)₂ (M = Na, K) Calcium Phosphate Bioceramics in Model Solutions. *Inorg. Mater.* **2018**, *54*, 500–508. [[CrossRef](#)]
5. Karapetyants, M.H.; Drakin, S.I. *General and Inorganic Chemistry*; Khimiya: Moscow, Russia, 1981; pp. 229–287. (In Russian)
6. Safronova, T.V.; Putlyayev, V.I. Medical Inorganic Materials Research in Russia: Calcium Phosphate Materials. *Nanosist. Fiz. Khim. Mat.* **2013**, *4*, 24–47. Available online: <https://www.elibrary.ru/item.asp?id=18964052> (accessed on 18 April 2022). (In Russian)
7. Winkler, T.; Sass, F.A.; Duda, G.N.; Schmidt-Bleek, K. A review of biomaterials in bone defect healing, remaining shortcomings and future opportunities for bone tissue engineering. *Bone Jt. Res.* **2018**, *7*, 232–243. [[CrossRef](#)]
8. Lin, F.H.; Liao, C.J.; Chen, K.S.; Sun, J.S.; Liu, H.C. Degradation behaviour of a new bioceramic: Ca₂P₂O₇ with addition of Na₄P₂O₇·10H₂O. *Biomaterials* **1997**, *18*, 915–921. [[CrossRef](#)]
9. Safronova, T.V.; Putlyayev, V.I.; Knot'ko, A.V.; Krut'ko, V.K.; Musskaya, O.N.; Ulasevich, S.A.; Vorob'eva, N.A.; Telitsin, V.D. Calcium Phosphate Ceramic in the System Ca(PO₃)₂-Ca₂P₂O₇ Based on Powder Mixtures Containing Calcium Hydrophosphate. *Glass Ceram.* **2018**, *75*, 279–286. [[CrossRef](#)]
10. Safronova, T.V.; Sadilov, I.S.; Chaikun, K.V.; Shatalova, T.B.; Filippov, Y.Y. Synthesis of Monetite from Calcium Hydroxyapatite and Monocalcium Phosphate Monohydrate under Mechanical Activation Conditions. *Russ. J. Inorg. Chem.* **2019**, *64*, 1088–1094. [[CrossRef](#)]
11. Safronova, T.V.; Putlayev, V.I.; Bessonov, K.A.; Ivanov, V.K. Ceramics based on calcium pyrophosphate nanopowders. *Process. Appl. Ceram.* **2013**, *7*, 9–14. [[CrossRef](#)]
12. Safronova, T.V.; Kurbatova, S.A.; Shatalova, T.B.; Knotko, A.V.; Yevdokimov, P.V.; Putlyayev, V.I. Calcium Pyrophosphate Powder for Production of Bioceramics Synthesized from Pyrophosphoric Acid and Calcium Acetate. *Inorg. Mater. Appl. Res.* **2017**, *8*, 118–125. [[CrossRef](#)]
13. Li, Y.Y.; Yang, D.A.; Zhao, H. Degradation behavior of β -Ca₃(PO₄)₂/ β -Ca₂P₂O₇ bioceramics. *Key Eng. Mater.* **2007**, *336*, 1650–1653. [[CrossRef](#)]

14. Safronova, T.V.; Shatalova, T.B.; Tikhonova, S.A.; Filippov, Y.Y.; Krut'ko, V.K.; Musskaya, O.N.; Kononenko, N.E. Synthesis of Calcium Pyrophosphate Powders from Phosphoric Acid and Calcium Carbonate. *Inorg. Mater. Appl. Res.* **2021**, *12*, 986–992. [[CrossRef](#)]
15. BernacheAssollant, D.; Ababou, A.; Champion, E.; Heughebaert, M. Sintering of calcium phosphate hydroxyapatite $\text{Ca}_{10}(\text{PO}_4)_6(\text{OH})_2$. I. Calcination and particle growth. *J. Eur. Ceram. Soc.* **2003**, *23*, 229–241. [[CrossRef](#)]
16. Hill, W.L.; Faust, G.T.; Reynolds, D.S. The binary system P_2O_5 ; $2\text{CaO}\cdot\text{P}_2\text{O}_5$. *Am. J. Sci.* **1944**, *242*, 457–477. [[CrossRef](#)]
17. Safronova, T.V.; Putlyaev, V.I. Powder systems for calcium phosphate ceramics. *Inorg. Mater.* **2017**, *53*, 17–26. [[CrossRef](#)]
18. Champion, E. Sintering of calcium phosphate bioceramics. *Acta Biomater.* **2013**, *9*, 5855–5875. [[CrossRef](#)]
19. Cacciotti, I.; Bianco, A.; Lombardi, M.; Montanaro, L. Mg-substituted hydroxyapatite nanopowders: Synthesis, thermal stability and sintering behaviour. *J. Eur. Ceram. Soc.* **2009**, *29*, 2969–2978. [[CrossRef](#)]
20. Yedekçi, B.; Tezcaner, A.; Alshemary, A.Z.; Yılmaz, B.; Demir, T.; Evis, Z. Synthesis and sintering of B, Sr, Mg multi-doped hydroxyapatites: Structural, mechanical and biological characterization. *J. Mech. Behav. Biomed. Mater.* **2021**, *115*, 104230. [[CrossRef](#)]
21. German, R.M.; Suri, P.; Park, S.J. Review: Liquid phase sintering. *J. Mater. Sci.* **2009**, *44*, 1–39. [[CrossRef](#)]
22. Lin, F.H.; Lin, C.C.; Lu, C.M.; Liu, H.C.; Sun, J.S.; Wang, C.Y. Mechanical properties and histological evaluation of sintered $\beta\text{-Ca}_2\text{P}_2\text{O}_7$ with $\text{Na}_4\text{P}_2\text{O}_7\cdot 10\text{H}_2\text{O}$ addition. *Biomaterials* **1995**, *16*, 793–802. [[CrossRef](#)]
23. Safronova, T.V.; Sadilov, I.S.; Chaikun, K.V.; Shatalova, T.B.; Filippov, Y.Y. Ceramics Based on a Powder Mixture of Calcium Hydroxyapatite, Monocalcium Phosphate Monohydrate, and Sodium Hydrogen Phosphate Homogenized under Mechanical Activation Conditions. *Inorg. Mater. Appl. Res.* **2020**, *11*, 879–885. [[CrossRef](#)]
24. Safronova, T.V.; Putlyaev, V.I.; Filippov, Y.Y.; Shatalova, T.B.; Naberezhnyi, D.O.; Nasridinov, A.F.; Larionov, D.S. Ceramics Based on Powder Mixtures Containing Calcium Hydrogen Phosphates and Sodium Salts (Na_2CO_3 , $\text{Na}_4\text{P}_2\text{O}_7$, and NaPO_3). *Inorg. Mater.* **2018**, *54*, 724–735. [[CrossRef](#)]
25. Safronova, T.V.; Putlyaev, V.I.; Filippov, Y.Y.; Shatalova, T.B.; Fatin, D.S. Ceramics Based on Brushite Powder Synthesized from Calcium Nitrate and Disodium and Dipotassium Hydrogen Phosphates. *Inorg. Mater.* **2018**, *54*, 195–207. [[CrossRef](#)]
26. Safronova, T.V.; Korneichuk, S.A.; Shatalova, T.B.; Lukina, Y.S.; Sivkov, S.P.; Filippov, Y.Y.; Krut'ko, V.K.; Musskaya, O.N. $\text{Ca}_2\text{P}_2\text{O}_7\text{-Ca}(\text{PO}_3)_2$ Ceramic Obtained by Firing β -Tricalcium Phosphate and Monocalcium Phosphate Monohydrate Based Cement Stone. *Glass Ceram.* **2020**, *77*, 165–172. [[CrossRef](#)]
27. Safronova, T.V.; Shatalova, T.B.; Filippov, Y.Y.; Krut'ko, V.K.; Musskaya, O.N.; Safronov, A.S.; Toshev, O.U. Ceramics in the $\text{Ca}_2\text{P}_2\text{O}_7\text{-Ca}(\text{PO}_3)_2$ System Obtained by Annealing of the Samples Made from Hardening Mixtures Based on Calcium Citrate Tetrahydrate and Monocalcium Phosphate Monohydrate. *Inorg. Mater. Appl. Res.* **2020**, *11*, 777–786. [[CrossRef](#)]
28. Safronova, T.V.; Korneichuk, S.A.; Putlyaev, V.I.; Boitsova, O.V. Ceramics made from calcium hydroxyapatite synthesized from calcium acetate and potassium hydrophosphate. *Glass Ceram.* **2008**, *65*, 131–135. [[CrossRef](#)]
29. Bibikov, V.Y.; Smirnov, V.V.; Fadeeva, I.V.; Rau, D.; Ferro, D.; Barinov, S.M.; Shvorneva, L.I. Intensification of Sintering of Carbonate-Hydroxyapatite Ceramics for Bone Implants. *Perspect. Mater.* **2005**, *6*, 43–48. Available online: <https://www.elibrary.ru/item.asp?id=19417615> (accessed on 18 April 2022). (In Russian).
30. Shiryaev, M.; Safronova, T.; Putlyaev, V. Calcium phosphate powders synthesized from calcium chloride and potassium hydrophosphate. *J. Therm. Anal. Calorim.* **2010**, *101*, 707–713. [[CrossRef](#)]
31. Safronova, T.V.; Putlyaev, V.I.; Shekhirev, M.A.; Tretyakov, Y.D.; Kuznetsov, A.V.; Belyakov, A.V. Densification additives for hydroxyapatite ceramics. *J. Eur. Ceram. Soc.* **2009**, *29*, 1925–1932. [[CrossRef](#)]
32. Safronova, T.V. Inorganic Materials for Regenerative Medicine. *Inorg. Mater.* **2021**, *57*, 443–474. [[CrossRef](#)]
33. Safronova, T.V.; Mukhin, E.A.; Putlyaev, V.I.; Knotko, A.V.; Evdokimov, P.V.; Shatalova, T.B.; Filippov, Y.Y.; Sidorov, A.V.; Karpushkin, E.A. Amorphous calcium phosphate powder synthesized from calcium acetate and polyphosphoric acid for bioceramics application. *Ceram. Int.* **2017**, *43*, 1310–1317. [[CrossRef](#)]
34. Zobel, D.; Ba, N. Untersuchungen zur Phosphitpyrolyse; Reaktionen beim Erhitzen von $\text{CaH}_2(\text{HPO}_3)_2\cdot\text{H}_2\text{O}$ in Abwesenheit von Sauerstoff. *Z. Chem.* **1969**, *9*, 433. [[CrossRef](#)]
35. Jackson, L.E.; Wright, A.J. A New Synthetic Route to Calcium Polyphosphates. *Key Eng. Mater.* **2005**, *284–286*, 71–74. [[CrossRef](#)]
36. Trommer, J.; Schneider, M.; Worzala, H.; Fitch, A.N. Structure determination of $\text{CaH}_2\text{P}_2\text{O}_7$ from in situ powder diffraction data. *Mater. Sci. Forum* **2000**, *321*, 374–379. [[CrossRef](#)]
37. Hossner, L.R.; Melton, J.R. Pyrophosphate Hydrolysis of Ammonium, Calcium, and Calcium Ammonium Pyrophosphates in Selected Texas Soils. *Soil Sci. Soc. Am. J.* **1970**, *34*, 801–805. [[CrossRef](#)]
38. Brown, E.H.; Brown, W.E.; Lehr, J.R.; Smith, J.P.; Frazier, A.W. Calcium ammonium pyrophosphates. *J. Phys. Chem.* **1958**, *62*, 366–367. [[CrossRef](#)]
39. Safronova, T.V.; Kiselev, A.S.; Shatalova, T.B.; Filippov, Y.Y.; Gavlina, O.T. Synthesis of double ammonium'calcium pyrophosphate monohydrate $\text{Ca}(\text{NH}_4)_2\text{P}_2\text{O}_7\cdot\text{H}_2\text{O}$ as the precursor of biocompatible phases of calcium phosphate ceramics. *Russ. Chem. Bull.* **2020**, *69*, 139–147. [[CrossRef](#)]
40. Subbarao, Y.V.; Ellis, R., Jr. Reaction products of polyphosphates and orthophosphates with soils and influence on uptake of phosphorus by plants. *Soil Sci. Soc. Am. J.* **1975**, *39*, 1085–1088. [[CrossRef](#)]
41. Brown, E.H.; Lehr, J.R.; Smith, J.P.; Frazier, A.W. Fertilizer Materials, Preparation and Characterization of Some Calcium Pyrophosphates. *J. Agric. Food Chem.* **1963**, *11*, 214–222. [[CrossRef](#)]

42. MacLennan, G.; Beevers, C.A. The crystal structure of monocalcium phosphate monohydrate, $\text{Ca}(\text{H}_2\text{PO}_4)_2 \cdot \text{H}_2\text{O}$. *Acta Cryst.* **1956**, *9*, 187–190. [[CrossRef](#)]
43. Boonchom, B.; Danvirutai, C. The Morphology and Thermal Behavior of Calcium Dihydrogen Phosphate Monohydrate ($\text{Ca}(\text{H}_2\text{PO}_4)_2 \cdot \text{H}_2\text{O}$) Obtained by a Rapid Precipitation Route at Ambient Temperature in Different Media. *J. Optoelectron. Biomed. Mater.* **2009**, *1*, 115–123. Available online: <https://chalcogen.ro/1Boonchom1.pdf> (accessed on 18 April 2022).
44. Safronova, T.V.; Paianidi, Y.A.; Shatalova, T.B.; Filippov, Y.Y.; Kazakova, G.K.; Umirov, U.T.; Toshev, O.U. Preparation of calcium polyphosphate powder containing amorphous carbon. *J. Ind. Chem. Soc.* **2020**, *97*, 2106–2110. [[CrossRef](#)]
45. ICDD. *International Centre for Diffraction Data*; Kabekkodu, S., Ed.; PDF-4+ 2010 (Database); ICDD: Newtown Square, PA, USA, 2010. Available online: <https://www.icdd.com/pdf-2/> (accessed on 20 February 2022).
46. Poltavtseva, R.A.; Pavlovich, S.V.; Klimantsev, I.V.; Tyutyunnik, N.V.; Grebennik, T.K.; Nikolaeva, A.V.; Sukhikh, G.T.; Nikonova, Y.A.; Selezneva, I.I.; Yaroslavtseva, A.K.; et al. Mesenchymal stem cells from human dental pulp: Isolation, characteristics, and potencies of targeted differentiation. *Bull. Exp. Biol. Med.* **2014**, *158*, 164–169. [[CrossRef](#)] [[PubMed](#)]
47. Tamimi, F.; Sheikh, Z.; Barralet, J. Dicalcium phosphate cements: Brushite and monetite. *Acta Biomater.* **2012**, *8*, 474–487. [[CrossRef](#)]
48. Jokić, B.; Mitrić, M.; Radmilović, V.; Drmanić, S.; Petrović, R.; Janačković, D. Synthesis and characterization of monetite and hydroxyapatite whiskers obtained by a hydrothermal method. *Ceram. Int.* **2011**, *37*, 167–173. [[CrossRef](#)]
49. Kanunnikova, O.M.; Mikhailova, S.S.; Mukhgalin, V.V.; Aksenova, V.V.; Gilmutdinov, F.Z.; Ladyanov, V.I. Structural and Chemical Transformations of the Mechanoactivated Calcium Lactate in Vortex Mill. *Chem. Phys. Mesoscopy* **2013**, *15*, 398–403. Available online: <https://elibrary.ru/item.asp?id=20285381> (accessed on 18 April 2022).
50. Sakata, Y.; Shiraishi, S.; Otsuka, M. Characterization of dehydration and hydration behavior of calcium lactate pentahydrate and its anhydrate. *Colloids Surf. B Biointerfaces* **2005**, *46*, 135–141. [[CrossRef](#)]
51. Bolhuis, G.K.; Eissens, A.C.; Zoestbergen, E. DC Calcium lactate, a new filler-binder for direct compaction of tablets. *Int. J. Pharm.* **2001**, *221*, 77–86. [[CrossRef](#)]
52. Polat, S. Thermal degradation of calcium lactate pentahydrate using TGA/FTIR/MS: Thermal kinetic and thermodynamics studies. *Indian Chem. Eng.* **2021**, 1–14. [[CrossRef](#)]
53. Fisher, C.H.; Filachione, E.M. *Properties and Reactions of Lactic Acid*; Eastern Regional Research Laboratory, Bureau of Agricultural and Industrial Chemistry, Agricultural Research Administration, United States Department of Agriculture: Philadelphia, PA, USA, 1950. Available online: <https://archive.org/details/propertiesreacti279fish/page/n1/mode/2up?view=theater> (accessed on 18 April 2022).
54. Serena, S.; Carbajal, L.; Sainz, M.A.; Caballero, A. Thermodynamic Assessment of the System $\text{CaO}-\text{P}_2\text{O}_5$: Application of the Ionic Two-Sublattice Model to Glass-Forming Melts. *J. Am. Ceram. Soc.* **2011**, *94*, 3094–3103. [[CrossRef](#)]
55. Pavlushkin, N.M. *Chemical Technology of Glass and Glassceramics*; Stroyizdat: Moscow, Russia, 1983; p. 428.